

Computational Approaches to Guide Pathogen Control Within Wildlife Reservoirs

A Dissertation

Presented in Partial Fulfillment of the Requirements for the

Degree of Doctor of Philosophy

with a

Major in Bioinformatics and Computational Biology

in the

College of Graduate Studies

University of Idaho

by

Tanner J. Varrelman

Major Professor: Christopher H. Remien, Ph.D.

Committee Members: James A. Foster, Ph.D.; Paul E. Gessler, Ph.D.;  
Paul Hohenlohe, Ph.D.; Stephen M. Krone, Ph.D.; Scott L. Nuismer, Ph.D.

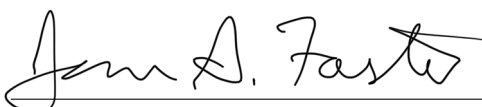
Department Administrator: David C. Tank, Ph.D.

May 2021

## AUTHORIZATION TO SUBMIT DISSERTATION

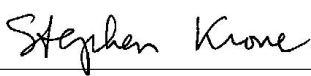
This dissertation of Tanner J. Varrelman, submitted for the degree of Doctor of Philosophy with a Major in Bioinformatics and Computational Biology and titled “Computational Approaches to Guide Pathogen Control Within Wildlife Reservoirs,” has been reviewed in final form. Permission, as indicated by the signatures and dates below is now granted to submit final copies for the College of Graduate Studies for approval.


Advisor:  4/19/21  
 Christopher H. Remien, Ph.D. Date

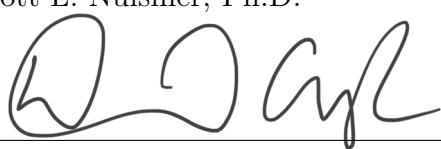
Committee Members:  4/22/21  
 James A. Foster, Ph.D. Date

 4/22/2021  
 Paul E. Gessler, Ph.D. Date

 4/22/2021  
 Paul Hohenlohe, Ph.D. Date

 4/22/2021  
 Stephen M. Krone, Ph.D. Date

 4/20/21  
 Scott L. Nuismer, Ph.D. Date

Department Chair:  4-23-21  
 David C. Tank, Ph.D. Date

## ABSTRACT

Zoonotic spillover is an ever-growing threat to human health, emphasizing the need for effective virus control measures within wildlife reservoirs. This dissertation explores the possibility for novel virus control measures and develops an open source Lassa virus database. In the first Chapter, we develop a mathematical model to evaluate the effectiveness of a transmissible vaccine within a heterogeneous wildlife population. Generally, we find that transmissible vaccines do not benefit from heterogeneity in vaccine transmission. Next, we model the spread of a transmissible vaccine constructed from a betaherpesvirus vector, a leading vector candidate for vaccine development. We find that a transmissible vaccine constructed from such a vector can reduce certain zoonotic pathogens within a year of vaccine introduction. Finally, we construct a database characterizing Lassa virus infection and sequence data as well as interactive tools for data visualization and management to facilitate research on Lassa virus in West Africa.

## ACKNOWLEDGEMENTS

I would like to thank Dr. Christopher Remien and Dr. Scott Nuismer for their continuous support while I completed this dissertation. Being a research assistant and graduate student under their leadership and mentorship has been invaluable to my development as a researcher. I would also like to thank Dr. Andrew Basinski, as his help has contributed greatly to the quality of this dissertation. Further, I thank the Nuismer lab as a whole for the great conversations and support over the past years. Finally, I would like to thank my graduate committee for the helpful suggestions and contributions to this work.

This study was funded by NIH [grant number R01GM122079] (S.L.N.) and DARPA [D18AC00028](S.L.N.).

## DEDICATION

I dedicate my dissertation work to my family. My parents, Benjamin and Jennifer Varrelman, have always put my sisters and I first and provide us with unconditional love, support, and encouragement. Without the support of my sisters, Madeline and Samantha, I would not be where I am today.

## TABLE OF CONTENTS

AUTHORIZATION TO SUBMIT THESIS . . . . .	ii
ABSTRACT . . . . .	iii
ACKNOWLEDGEMENTS . . . . .	iv
DEDICATION . . . . .	v
TABLE OF CONTENTS . . . . .	vi
LIST OF TABLES . . . . .	viii
LIST OF FIGURES . . . . .	ix
CHAPTER 1: TRANSMISSIBLE VACCINES IN HETEROGENEOUS POPULATIONS: IM- PLICATIONS FOR VACCINE DESIGN . . . . .	1
ABSTRACT . . . . .	1
INTRODUCTION . . . . .	1
METHODS . . . . .	3
RESULTS . . . . .	9
DISCUSSION . . . . .	18
CONCLUSION . . . . .	20
APPENDIX . . . . .	21
CHAPTER 2: THE ZOONOSES END GAME: QUANTIFYING THE EFFECTIVENESS OF BETAHERPESVIRUS-VECTORED TRANSMISSIBLE VACCINES . . . . .	30
ABSTRACT . . . . .	30
INTRODUCTION . . . . .	30
RESULTS . . . . .	32
DISCUSSION . . . . .	41
METHODS . . . . .	43
SUPPLEMENTAL INFORMATION . . . . .	48

CHAPTER 3: FACILITATING OPEN SCIENCE IN LASSA VIRUS RESEARCH . . . . .	56
ABSTRACT . . . . .	56
INTRODUCTION . . . . .	56
METHODS . . . . .	57
RESULTS . . . . .	60
DISCUSSION . . . . .	65
REFERENCES . . . . .	68

## LIST OF TABLES

1.1	Model state variables and parameters. Subscript $i$ specifies the subgroup of the population. . . . .	7
2.1	MCMV parameter estimates found using a combination of Approximate Bayesian Computation and steady-state methods. It is important to note that the N1 strain was not found in any of the natural populations that were sampled across Australia, therefore our only N1 sample comes from the enclosure study. Further, to account for possible sampling error during the capture of rodents, we calculated the Clopper–Pearson 95% confidence interval on the MCMV sampling data, and then calculated the $\beta_v$ estimate. To be conservative in our parameter estimate, we used the minimum value from the confidence interval. . . . .	40
2.2	The possible events, transitions, and transition rates found in the CTMC model. . .	50
2.3	Prior distributions for each parameter in the MCMV model. . . . .	52
3.1	Sample locations of Lassa virus prevalence data. Currently, the viral infection data set consists of human serosurveys from 94 locations, and rodent serology and virus extraction from 80 locations. . . . .	61
3.2	Number of Lassa virus sequences sampled from each of the eight countries represented in the data set. Not all samples represented in this table are present in our mapping, as a large majority of sequences lack an associated latitude and longitude. . . . .	63



## LIST OF FIGURES

- 1.1 Transmission events in the mathematical model. Subgroup one is assumed to maintain high within subgroup pathogen transmission (left), and subgroup two is assumed to maintain a low level of within subgroup pathogen transmission (right). High and low vaccine transmission is determined by the assumed vaccine design. Vaccine and pathogen-infected individuals can infect susceptible individuals within their subgroup  $(\beta_{v,1,1}, \beta_{v,2,2}, \beta_{w,1,1}, \beta_{w,2,2})$ , as well as susceptible individuals in the other subgroup, at a reduced rate  $(\beta_{v,1,2}, \beta_{v,2,1}, \beta_{w,1,2}, \beta_{w,2,1})$ . . . . . 6
- 1.2 Vaccination threshold required to prevent pathogen invasion when using a transmissible vaccine (shown by the blue line), and traditional vaccine (shown by the orange line). Each panel depicts the vaccination threshold, for low and high heterogeneity in transmission, and correlation in transmission. Within subgroup  $R_0$  values of the vaccine and pathogen are depicted in the inset bar plot. Top panels: Global  $R_{0,w} = 3.697$ , global  $R_{0,v} = 0.880$ . Bottom panels: Global  $R_{0,w} = 4.193$ , global  $R_{0,v} = 0.998$ . Fractional reduction in vaccination effort afforded by a transmissible vaccine (clockwise, starting in the top left panel): a.) Optimal strategy=0.24, Random strategy=0.24, b.) Optimal strategy=0.25, Random strategy=0.22, c.) Optimal strategy=0.31, Random strategy=0.15, d.) Optimal strategy=0.25, Random strategy=0.25. Parameters varied across panels: a.)  $R_{0,v,1,1}=0.7$ ,  $R_{0,v,2,2}=0.5$ ,  $R_{0,w,1,1}=2.94$ ,  $R_{0,w,2,2}=2.1$ , b.)  $R_{0,v,1,1}=0.5$ ,  $R_{0,v,2,2}=0.7$ ,  $R_{0,w,1,1}=2.94$ ,  $R_{0,w,2,2}=2.1$ , c.)  $R_{0,v,1,1}=0.3$ ,  $R_{0,v,2,2}=0.9$ ,  $R_{0,w,1,1}=3.78$ ,  $R_{0,w,2,2}=1.26$ , d.)  $R_{0,v,1,1}=0.9$ ,  $R_{0,v,2,2}=0.3$ ,  $R_{0,w,1,1}=3.78$ ,  $R_{0,w,2,2}=1.26$ . Parameters conserved across panels:  $\gamma=0.02$ ,  $d=0.01$ ,  $b_1=10$ ,  $b_2=10$ ,  $R_{0,v,1,2}=0.26$ ,  $R_{0,v,2,1}=0.26$ ,  $R_{0,w,1,2}=1.1$ ,  $R_{0,w,2,1}=1.1$ . . . . . 11

1.3 The fractional reduction in prophylaxis vaccination effort for both vaccine designs and strategies. We hold the vaccine  $R_0$  constant, and proportionally increase the pathogen transmission parameters, allowing us to look at a range of global  $R_{0,w}$  values. Parameter values are as followed: (Top panels) Vaccine transmission positive correlation:  $R_{0,v,1,1}=0.45$ ,  $R_{0,v,2,2}=0.27$ ,  $R_{0,v,1,2}=0.18$ ,  $R_{0,v,2,1}=0.18$ , Vaccine transmission negative correlation:  $R_{0,v,1,1}=0.27$ ,  $R_{0,v,2,2}=0.45$ ,  $R_{0,v,1,2}=0.18$ ,  $R_{0,v,2,1}=0.18$ , Pathogen transmission:  $R_{0,w,1,1}=\text{range}(0.91-3.63)$ ,  $R_{0,w,2,2}=\text{range}(0.54-2.17)$ ,  $R_{0,w,1,2}=\text{range}(0.36-1.44)$ ,  $R_{0,w,2,1}=\text{range}(0.36-1.44)$ . (Bottom panels) Vaccine transmission positive correlation:  $R_{0,v,1,1}=0.54$ ,  $R_{0,v,2,2}=0.18$ ,  $R_{0,v,1,2}=0.18$ ,  $R_{0,v,2,1}=0.18$ , Vaccine transmission negative correlation:  $R_{0,v,1,1}=0.18$ ,  $R_{0,v,2,2}=0.54$ ,  $R_{0,v,1,2}=0.18$ ,  $R_{0,v,2,1}=0.18$ , Pathogen transmission:  $R_{0,w,1,1}=\text{range}(1.09-4.35)$ ,  $R_{0,w,2,2}=\text{range}(0.36-1.45)$ ,  $R_{0,w,1,2}=\text{range}(0.36-1.44)$ ,  $R_{0,w,2,1}=\text{range}(0.36-1.44)$ . Parameters conserved across panels:  $\gamma=0.02$ ,  $d=0.01$ ,  $b_1=10$ ,  $b_2=10$ . . . . . 13

1.4 The proportional reduction in pathogen incidence attributed to vaccine transmission for a vaccine experiencing negative and positive correlation with respect to heterogeneity in pathogen transmission. Top panel: Global  $R_{0,w} = 3.70$ , global  $R_{0,v} = .88$ . Bottom panel: Global  $R_{0,w} = 4.19$ , global  $R_{0,v} = 1.00$ . Note that although the average within subgroup transmission remains constant, increasing heterogeneity increases the  $R_0$  of the infectious agents. Parameter values used in the figure: (Top panel) Vaccine transmission w/ positive correlation:  $R_{0,v,1,1}=0.7$ ,  $R_{0,v,2,2}=0.5$ , Vaccine transmission w/ negative correlation:  $R_{0,v,1,1}=0.5$ ,  $R_{0,v,2,2}= 0.7$ , Pathogen transmission:  $R_{0,w,1,1}=2.94$ ,  $R_{0,w,2,2}=2.1$ . (Bottom Panel) Vaccine transmission w/ positive correlation:  $R_{0,v,1,1}=0.9$ ,  $R_{0,v,2,2}=0.3$ , Vaccine transmission w/ negative correlation:  $R_{0,v,1,1}=0.3$ ,  $R_{0,v,2,2}=0.9$ , Pathogen transmission:  $R_{0,w,1,1}=3.78$ ,  $R_{0,w,2,2}=1.26$ . Parameters conserved across panels:  $\bar{\sigma}=0.4$ ,  $\gamma=0.02$ ,  $d=0.01$ ,  $b_1=10$ ,  $b_2=10$ ,  $R_{0,v,1,2}=0.26$ ,  $R_{0,v,2,1}=0.26$ ,  $R_{0,w,1,2}=1.1$ ,  $R_{0,w,2,1}=1.1$ . . . . . 15

- 1.5 Proportion of male/female deer mice that must be vaccinated for prophylaxis against Sin Nombre Virus. The pathogen maintains a global  $R_{0,w} = 1.21$ , and two possible vaccine designs maintaining a global  $R_{0,v} = 0.61$ . The gray region provides a reference for typical values of the proportion of individuals successfully vaccinated in a wildlife vaccination campaign (see Appendix: SNV Invasion in Deer Mice). Fractional reduction in vaccination effort provided by a transmissible vaccine (left to right): a.) Optimal strategy=0.47, Random strategy=0.52, b.) Optimal strategy=0.24, Random strategy=0.38. Parameters: a.)  $R_{0,v,1,1}=0.53$ ,  $R_{0,v,2,2}=0.18$ ,  $R_{0,v,1,2}=0.18$ ,  $R_{0,v,2,1}=0.18$ ,  $R_{0,w,1,1}=1.06$ ,  $R_{0,w,2,2}=0.36$ ,  $R_{0,w,1,2}=0.36$ ,  $R_{0,w,2,1}=0.36$ , b.)  $R_{0,v,1,1}=0.18$ ,  $R_{0,v,2,2}=0.53$ ,  $R_{0,v,1,2}=0.18$ ,  $R_{0,v,2,1}=0.18$ ,  $R_{0,w,1,1}=1.06$ ,  $R_{0,w,2,2}=0.36$ ,  $R_{0,w,1,2}=0.36$ ,  $R_{0,w,2,1}=0.36$ . 18
- 2.1 Bivariate posterior distribution of the transmission rate ( $\beta_v$ ) and the rate at which individuals exposed to the virus transition into the infectious class ( $\alpha_1$ ). The marginal distribution of the transmission rate and rate of becoming infectious are displayed on the top and right of the density plot, respectively. The modal values of the distribution are as followed:  $\beta_v = 0.033$  individual<sup>-1</sup> day<sup>-1</sup>,  $\alpha_1 = 0.099$  day<sup>-1</sup>. . . . 33
- 2.2 Time to ninety-five percent pathogen reduction as a function of pathogen  $R_0$  and the infectious period ( $1/\gamma$ ). Simulations start at the steady state quantities for susceptible and pathogen infected individuals, and 10% of the susceptible population is exposed to the transmissible vaccine. The pathogens highlighted in this figure include Lassa virus (LASV) and Lymphocytic Choriomeningitis virus (LCMV). . . . 34

- 2.3 Temporal dynamics of (a) Lassa virus (LASV) and (b) Lymphocytic Choriomenin-  
gitis virus (LCMV) reduction as a result of using a MCMV-vectored transmissible  
vaccine. Simulations are initialized at the steady state quantities for susceptible  
and pathogen infected individuals, with 10% of the susceptible population removed  
and exposed to the transmissible vaccine. For each pathogen example we randomly  
sampled  $\beta_v$  and  $\alpha_1$  from the posterior distribution 100 times, and simulated our  
model forward in time for each set of parameters. The grey region represents the  
100 simulations, where the orange dashed line is the mean. The grey vertical lines  
indicate the minimum, mean, and maximum time to 95% pathogen reduction ((a)  
min=121 days, mean=371 days, max=194 days (b) min=609 days, mean=701 days,  
max=940 days). . . . . 36
- 2.4 Temporal dynamics of (a) Lassa virus (LASV) and (b) Lymphocytic Choriomenin-  
gitis virus (LCMV) reduction as a result of using an MCMV-vectored transmissible  
vaccine with varying levels of efficacy. Simulations are initialized at the steady  
state quantities for susceptible and pathogen infected individuals, where 10% of the  
susceptible population is removed and exposed to the transmissible vaccine. . . . . 38
- 2.5 (a) Time to ninety-five percent pathogen reduction across four geographic locations.  
Simulations start at the steady state quantities for susceptible and pathogen infected  
individuals (see Supplementary Information), where 10% of the susceptible popula-  
tion is removed and exposed to the transmissible vaccine.  $R_{0,w} > R_{0,v}$  represents  
the scenario when the vaccine fails to reduce the pathogen. (b) Geographic locations  
represented in the data. . . . . 41
- 3.1 Structure of the Lassa data in the MySQL database. We create separate tables for  
the country names, the reference studies, the sequence data, and the infection data.  
Within the sequence and infection tables, there is a country\_id and reference\_id that  
point to the values found in the country and reference tables, respectively. Note,  
data fields within the sequence and infection table are omitted from this visualization. 59

3.2	a.) 94 sample locations from seven human serosurveys. b.) 80 sample locations for rodent serology and virus detection. Note that overlapping sample locations results in a darker band around the red data points. . . . .	62
3.3	Sample locations of viral sequences across West Africa. Our data set currently consists of 579 Lassa sequences that have spatially explicit meta data (85 from human hosts and 494 from rodent hosts). Note that overlapping sample locations results in a darker band around the orange data points. . . . .	64
3.4	Visualization of the Lassa virus dashboard. . . . .	65

# CHAPTER 1: TRANSMISSIBLE VACCINES IN HETEROGENEOUS POPULATIONS: IMPLICATIONS FOR VACCINE DESIGN

## 1.1 ABSTRACT

Transmissible vaccines may provide a promising solution for improving the control of infectious disease, particularly zoonotic pathogens with wildlife reservoirs. Although it is well known that heterogeneity in pathogen transmission impacts the spread of infectious disease, the effects of heterogeneity on vaccine transmission are largely unknown. Here we develop and analyze a mathematical model that quantifies the potential benefits of a transmissible vaccine in a population where transmission is heterogeneous between two subgroups. Our results demonstrate that the effect of heterogeneity on the benefit of vaccine transmission largely depends on the vaccine design and the pattern of vaccine administration across subgroups. Specifically, our results show that in most cases a transmissible vaccine designed to mirror the transmission of the pathogen is optimal. If the vaccination effort can be preferentially biased towards a given subgroup, a vaccine with a pattern of transmission opposite to that of the pathogen can become optimal in some cases. To better understand the consequences of heterogeneity on the effectiveness of a transmissible vaccine in the real world, we parameterized our model using data from Sin Nombre virus in deer mice (*Peromyscus maniculatus*). The results of this analysis reveal that when a vaccination campaign is limited in vaccine availability, a traditional vaccine must be administered primarily to males for the spread of Sin Nombre virus to be prevented. In contrast, a transmissible vaccine remains effective even when it cannot be preferentially administered to males.

## 1.2 INTRODUCTION

Zoonoses, particularly those circulating in wildlife populations, are a primary source of pathogens that infect humans [1]. The burden of such pathogens on human populations

can be profound, as demonstrated in the 2014-2015 West African Ebola virus epidemic. The virus was transmitted from wild animal populations such as fruit bats and apes [2], and resulted in over 11,000 human deaths and cost over 3.6 billion dollars [3]. Such outbreaks highlight the need to develop cost-effective strategies that mitigate zoonotic spillover into human populations. One strategy for reducing the spillover potential of zoonoses is to decrease the prevalence of infectious disease within wildlife reservoir populations. Both culling [4] and mass vaccination [4, 5] have been used to control pathogens in wildlife reservoir populations. Though both strategies have been successful in some cases [4], the costs of implementation and the difficulties of delivering vaccine to wild animals limit their scope of applicability [6]. Transmissible vaccines are a novel tool that might overcome some of these challenges, allowing for pathogen reduction or even the prevention of pathogen spread in wildlife reservoirs.

Transmissible vaccines, also known as self-disseminating vaccines, are live viral vaccines with the ability to transmit between hosts [7]. Mathematical models demonstrate that vaccine transmission reduces the vaccination effort required to protect a population [8], can reduce a pathogen's prevalence in a population, or facilitate pathogen eradication altogether [8–10]. Though insightful, these models simplify host biology by assuming that all hosts are identical in their capacity to transmit the vaccine and pathogen. In reality, of course, individual hosts differ in their transmission due to factors such as sex and age [11], and this heterogeneity in host populations has been shown to influence the outcome of vaccination campaigns as well as the optimal vaccination strategy [12]. For instance, if vaccine is delivered to a heterogeneous host population at random, pathogen control requires a greater rate of vaccination than in a uniform host population [12]. In contrast, if it is possible to deliver vaccine selectively or optimally, the vaccination rate required for pathogen control can actually be less in a heterogeneous host population than a homogeneous host population [12]. Preferentially distributing a vaccine to a super-spreading class increases the overall effectiveness of a vaccination campaign [11].

Unfortunately, effectively identifying super-spreaders and selectively delivering vaccine to them is a formidable and unresolved public health challenge in many systems [13].

Mathematical models of another transmissible therapy, therapeutic interfering particles (TIPs), have demonstrated that heterogeneity in host transmission increases the effectiveness of TIPs by autonomously targeting super-spreaders [13]. TIPs replicate only in the presence of the pathogen, and naturally follow the same transmission pathways [13]. In a similar fashion, transmissible vaccines may benefit from following the same transmission pathways as the pathogen, thus increasing their effectiveness in heterogeneous populations. Although intuitively appealing, it is unknown whether the benefits demonstrated for TIPs in heterogeneous host populations also occur for transmissible vaccines. Here we explore the effects of vaccine transmission in a host population with heterogeneity in vaccine and pathogen transmission (i.e., some individuals spread the infectious agent to a higher degree than others). To this end, we develop mathematical models to quantify the effectiveness of a transmissible vaccine in a host population composed of subgroups that transmit a vaccine and pathogen at different rates. Our analyses address three specific questions: 1.) How sensitive are the benefits of vaccine transmission to population-level heterogeneity? 2.) Do certain patterns of heterogeneity favor the use of a vaccine that mimics the biased spread of a pathogen? 3) Do levels of heterogeneity observed in a natural reservoir population (Sin Nombre virus (SNV) in deer mice (*Peromyscus maniculatus*)) significantly influence the effectiveness of a transmissible vaccine?

### 1.3 METHODS

We developed a model describing the spread of a pathogen and transmissible vaccine in a heterogeneous animal population. Hosts in the population fall into one of two subgroups. Each subgroup is defined by a unique set of parameters that reflect differences in the hosts' ability to transmit a pathogen and a transmissible vaccine. We assume that subgroup identity is a result of fixed differences in host biology (e.g., behavior, sex, genome), and



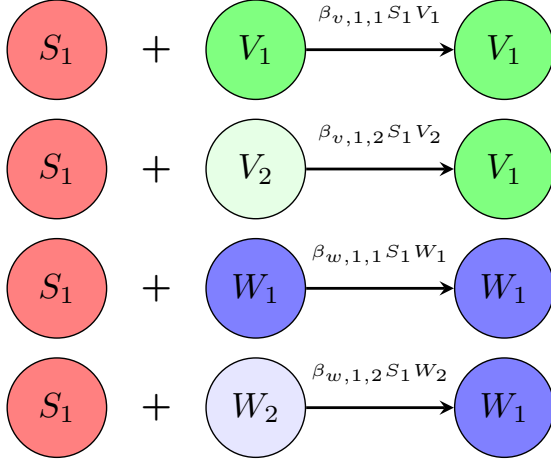
as a consequence, hosts remain in the subgroup into which they were born. Based on the classic Susceptible-Infected-Recovered (SIR) model of disease spread [14], individuals in each subgroup  $i$  are further partitioned into classes that reflect their immunological status to a transmissible vaccine and pathogen: susceptible to both pathogen and vaccine ( $S_i$ ), pathogen-infected ( $W_i$ ), vaccine-infected ( $V_i$ ), and recovered ( $R$ ). New susceptible individuals are introduced into subgroup  $i$  at a constant rate  $b_i$  and all individuals die at rate  $d$ . Although we refer to  $b_i$  as birth for simplicity, it more accurately describes the rate at which new susceptible individuals are added to the population through any mechanism. Susceptible individuals can be directly vaccinated as they are introduced into the susceptible class, or indirectly through infection with the vaccine. Although challenging in wildlife populations, direct vaccination of susceptible individuals may be possible in a number of ways. For instance, a captive colony could be used as a source of directly vaccinated juveniles, vaccine baits could be designed in a way that favors consumption by juvenile individuals more likely to be susceptible, or pregnant females could be targeted with vaccines capable of vertical transmission. In the model, a fraction  $\sigma_i$  of births into subgroup  $i$  are directly vaccinated and immediately enter the vaccine-infected class  $V_i$ .

The rate at which the vaccine and pathogen spread between susceptible and infected hosts depends on the subgroup identities of the hosts involved. The parameters  $\beta_{v,i,j}$  and  $\beta_{w,i,j}$  describe the rates of transmission from subgroup  $j$  to subgroup  $i$  for a transmissible vaccine and pathogen, respectively (Figure 1.1). For example, pathogen-infected individuals within subgroup  $j$  transmit the infection to susceptible individuals in subgroup  $i$  according to the mass-action rate  $\beta_{w,i,j}S_iW_j$ . Because susceptible individuals of subgroup  $i$  can become pathogen-infected by members of either subgroup, the total rate of pathogen infection in subgroup  $i$  is  $\sum_{j=1}^2 \beta_{w,i,j}S_iW_j$ . Upon pathogen infection, a susceptible in class  $S_i$  transitions to the pathogen-infected class  $W_i$ . Likewise, susceptible hosts in subgroup  $i$  become infected with the vaccine at rate  $\sum_{j=1}^2 \beta_{v,i,j}S_iV_j$ , and transition into class  $V_i$ . Because of the assumed immunological cross-reactivity between the vaccine

and the pathogen, individuals who experience infection from one agent are immune to future infections from either agent. Individuals who are infected with either the vaccine or pathogen recover at rate  $\gamma$ . Because recovered hosts no longer contribute to the infection process, we combine the subgroups into a common  $R$  class. A list of model variables and parameters can be found in Table 1.1. The resulting system of ordinary differential equations is:

$$\begin{aligned}
\frac{dS_i}{dt} &= b_i(1 - \sigma_i) - dS_i - \sum_{j=1}^2 (\beta_{v,i,j}S_iV_j + \beta_{w,i,j}S_iW_j) \\
\frac{dV_i}{dt} &= b_i\sigma_i - (\gamma + d)V_i + \sum_{j=1}^2 \beta_{v,i,j}S_iV_j \\
\frac{dW_i}{dt} &= -(\gamma + d)W_i + \sum_{j=1}^2 \beta_{w,i,j}S_iW_j \\
\frac{dR}{dt} &= -dR + \sum_{j=1}^2 (\gamma V_j + \gamma W_j).
\end{aligned} \tag{1.1}$$

### High Pathogen Transmission



### Low Pathogen Transmission

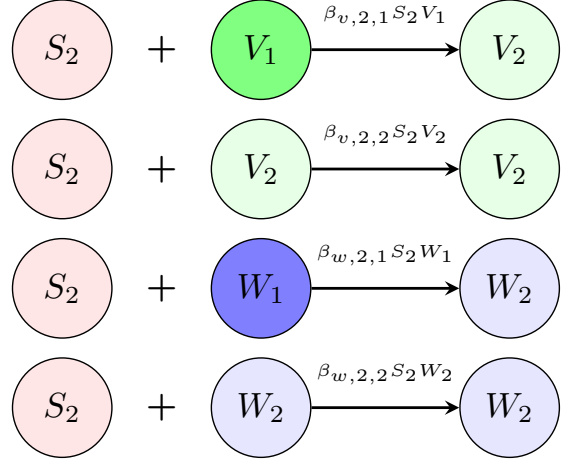


Figure 1.1: Transmission events in the mathematical model. Subgroup one is assumed to maintain high within subgroup pathogen transmission (left), and subgroup two is assumed to maintain a low level of within subgroup pathogen transmission (right). High and low vaccine transmission is determined by the assumed vaccine design. Vaccine and pathogen-infected individuals can infect susceptible individuals within their subgroup ( $\beta_{v,1,1}, \beta_{v,2,2}, \beta_{w,1,1}, \beta_{w,2,2}$ ), as well as susceptible individuals in the other subgroup, at a reduced rate ( $\beta_{v,1,2}, \beta_{v,2,1}, \beta_{w,1,2}, \beta_{w,2,1}$ ).

Name	Description	Units
$S_i$	Susceptible class	individuals
$V_i$	Vaccine-infected class	individuals
$W_i$	Disease infected individuals	individuals
$R$	Recovered individuals	individuals
$\beta_{v,i,j}$	Vaccine transmission rate from sub-group $j$ to $i$	individual <sup>-1</sup> day <sup>-1</sup>
$\beta_{w,i,j}$	Disease transmission rate from sub-group $j$ to $i$	individual <sup>-1</sup> day <sup>-1</sup>
$\gamma$	Recovery rate	day <sup>-1</sup>
$b_i$	Birth rates	day <sup>-1</sup>
$d$	Death rate	day <sup>-1</sup>
$R_{0,w}$	Disease reproductive number	nondimensional
$R_{0,v}$	Transmissible-vaccine reproductive number	nondimensional
$\sigma_i$	Proportion of newborns vaccinated directly	nondimensional
$\bar{\sigma}$	Average proportion of newborns that are directly vaccinated across groups	nondimensional
$\delta_\sigma$	Difference in the proportion of directly vaccinated newborns across groups	nondimensional

Table 1.1: Model state variables and parameters. Subscript  $i$  specifies the subgroup of the population.

To simplify our model, we make several assumptions regarding the transmission coefficients,  $\beta_{w,i,j}$  and  $\beta_{v,i,j}$ . First, we assume that for both infectious agents, within-group infectious contacts occur more frequently than between-group contacts. This assumption,

known as assortative mixing [15], can be expressed mathematically for the pathogen as  $\beta_{w,i,i} > \beta_{w,i,j}$  for  $i \neq j$ , and similarly for the vaccine. Without loss of generality, we assume subgroup 1 of the population spreads the pathogen to a greater extent than subgroup 2, so that  $\beta_{w,1,1} > \beta_{w,2,2}$ . In addition, we assume equal cross transmission between groups:  $\beta_{v,1,2} = \beta_{v,2,1}$  and  $\beta_{w,1,2} = \beta_{w,2,1}$ .

We focus on two possibilities of how the transmission rates of the vaccine relate to pathogen transmission between subgroups. In the first scenario, which we term positive correlation, the ordering of the vaccine transmission coefficients follows that of the pathogen, so that vaccine transmission is greatest in subgroup 1 ( $\beta_{v,1,1} > \beta_{v,2,2}$ ). Because the heterogeneity in vaccine transmission mimics that of the pathogen, this scenario is likely relevant for transmissible vaccines produced through pathogen attenuation. Although unintentional, the best example of an attenuated transmissible vaccine is the Oral Polio Vaccine (OPV), which quite likely follows the transmission pathways of wild type Polio [16]. The second scenario, which we term negative correlation, describes a transmissible vaccine that spreads better in the subgroup with low pathogen transmission, so that  $\beta_{v,1,1} < \beta_{v,2,2}$ . Although unlikely for an attenuated vaccine, this scenario is in principle possible for recombinant vector vaccines whose transmission is determined by a vector that is unrelated to the pathogen. Recombinant vector transmissible vaccines targeting Lassa fever in *Mastomys natalensis* and Ebola virus in primates are currently being developed using a Cytomegalovirus vector, and are likely to fall in this category [7, 17]. Focusing on these two potential vaccine characteristics, we evaluate the effectiveness of a transmissible vaccine in preventing pathogen invasion and in reducing pathogen incidence when vaccination prophylaxis cannot be achieved. We then parameterize our model using data from Sin Nombre virus to quantify the impact of vaccine transmission in a system that displays heterogeneity in pathogen transmission.

## 1.4 RESULTS

### PATHOGEN PROPHYLAXIS

A common goal of vaccination campaigns is to prevent a zoonotic pathogen from spreading to new populations that have not yet experienced infection. This is becoming particularly true for high impact zoonotic pathogens such as Ebola in great apes, rabies in a variety of reservoir species, and Lassa fever in rodent populations [7]. This goal is achieved by vaccinating the population to an extent that halts the spread of the targeted pathogen. In our model of a vaccination campaign,  $\sigma_1$  and  $\sigma_2$  denote the proportion of newborn individuals that are directly vaccinated in subgroups 1 and 2 respectively. We identify the threshold combinations of vaccination effort  $(\sigma_1, \sigma_2)$  that protect the entire population from pathogen invasion (Figure 1.2, Appendix: Pathogen Prophylaxis). Each panel of Figure 1.2 depicts the limiting combinations of direct vaccination that result in prophylaxis when a non-transmissible (orange curve) or transmissible vaccine (blue curve) is used. Along each threshold curve, we characterize two vaccination strategies: random and optimal. The random strategy applies to many real-world vaccination campaigns that, due to limited host access, cannot preferentially target one subgroup over another. Instead, the total vaccination effort  $(\sigma_1 + \sigma_2)$  is distributed equally between the subgroups so that  $\sigma_1 = \sigma_2$ . In contrast, the optimal vaccination strategy is the combination  $(\sigma_1, \sigma_2)$  that prevents pathogen invasion with the minimal amount of total vaccination effort.

Our results indicate that, across different levels of heterogeneity in transmission between the subgroups, and for both positively and negatively correlated vaccine designs, the use of a transmissible vaccine reduces the minimal vaccination effort needed to prevent pathogen invasion. This can be seen in Figure 1.2 by noting that the transmissible vaccination threshold (blue curve) is closer to the origin  $(\sigma_1 = \sigma_2 = 0)$  than the traditional vaccination threshold (orange curve). Consequently, the total amount of vaccination required to reach the prophylaxis threshold is smaller when a transmissible vaccine is used.

Comparing the optimal and random vaccination strategies along the prophylaxis threshold curves shows that for a population with high heterogeneity between subgroups, the optimal vaccination strategy biases vaccine distribution to the subgroup in which pathogen transmission is greatest. This bias in the optimal strategy is present regardless of whether the vaccine and pathogen transmission coefficients are positively correlated between the subgroups or negatively correlated between subgroups.

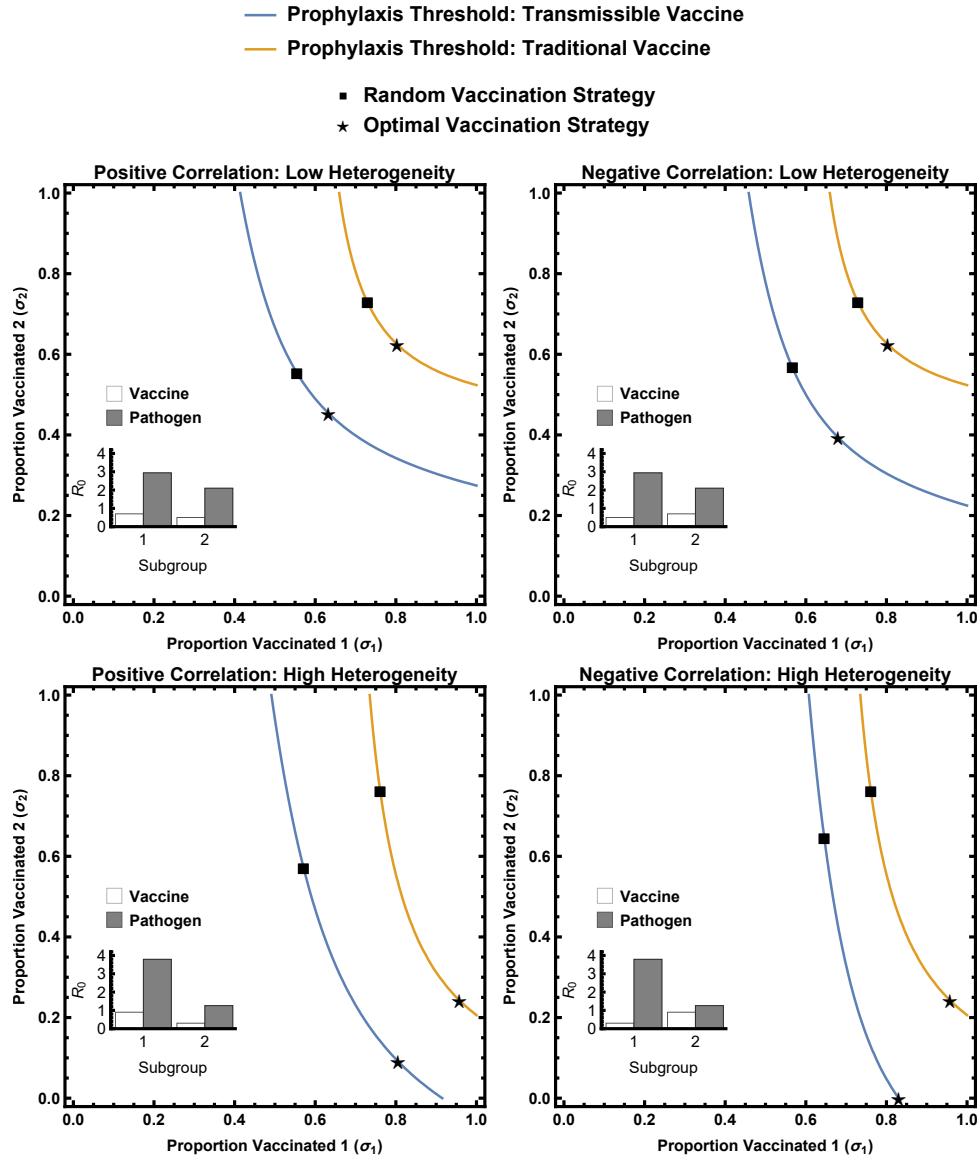


Figure 1.2: Vaccination threshold required to prevent pathogen invasion when using a transmissible vaccine (shown by the blue line), and traditional vaccine (shown by the orange line). Each panel depicts the vaccination threshold, for low and high heterogeneity in transmission, and correlation in transmission. Within subgroup  $R_0$  values of the vaccine and pathogen are depicted in the inset bar plot. Top panels: Global  $R_{0,w} = 3.697$ , global  $R_{0,v} = 0.880$ . Bottom panels: Global  $R_{0,w} = 4.193$ , global  $R_{0,v} = 0.998$ . Fractional reduction in vaccination effort afforded by a transmissible vaccine (clockwise, starting in the top left panel): a.) Optimal strategy=0.24, Random strategy=0.24, b.) Optimal strategy=0.25, Random strategy=0.22, c.) Optimal strategy=0.31, Random strategy=0.15, d.) Optimal strategy=0.25, Random strategy=0.25. Parameters varied across panels: a.)  $R_{0,v,1,1}=0.7$ ,  $R_{0,v,2,2}=0.5$ ,  $R_{0,w,1,1}=2.94$ ,  $R_{0,w,2,2}=2.1$ , b.)  $R_{0,v,1,1}=0.5$ ,  $R_{0,v,2,2}=0.7$ ,  $R_{0,w,1,1}=2.94$ ,  $R_{0,w,2,2}=2.1$ , c.)  $R_{0,v,1,1}=0.3$ ,  $R_{0,v,2,2}=0.9$ ,  $R_{0,w,1,1}=3.78$ ,  $R_{0,w,2,2}=1.26$ , d.)  $R_{0,v,1,1}=0.9$ ,  $R_{0,v,2,2}=0.3$ ,  $R_{0,w,1,1}=3.78$ ,  $R_{0,w,2,2}=1.26$ . Parameters conserved across panels:  $\gamma=0.02$ ,  $d=0.01$ ,  $b_1=10$ ,  $b_2=10$ ,  $R_{0,v,1,2}=0.26$ ,  $R_{0,v,2,1}=0.26$ ,  $R_{0,w,1,2}=1.1$ ,  $R_{0,w,2,1}=1.1$ .



Additionally, we evaluate which vaccine design is most beneficial when compared to a traditional vaccine, under both vaccination strategies (random and optimal) and across low and high levels of heterogeneity in transmission. To do so, we find the fractional reduction in the total vaccination relative a non-transmissible vaccine that is required to meet the prophylaxis threshold. Figure 1.3 shows the fractional reductions for both vaccination strategies and designs, across low and high levels of heterogeneity, when facing a range of global pathogen  $R_0$  values. Our results demonstrate that if a random vaccination strategy is applied, a positively correlated vaccine results in the greatest reduction in vaccination effort, relative to that of a non-transmissible vaccine (left column, Figure 1.3). Furthermore, for a fixed, average pathogen  $R_0$ , the fractional reduction from a positively correlated vaccine design remains relatively constant when heterogeneity is increased from low to high. In contrast, the benefit of a negatively correlated vaccine decreases as heterogeneity increases (Figure 1.3). Generally, these results suggest that when a random vaccination strategy is implemented, the benefit of a positively correlated vaccine design is robust under different levels of population heterogeneity. Negatively correlated designs, in contrast, work best when population heterogeneity is small or absent.

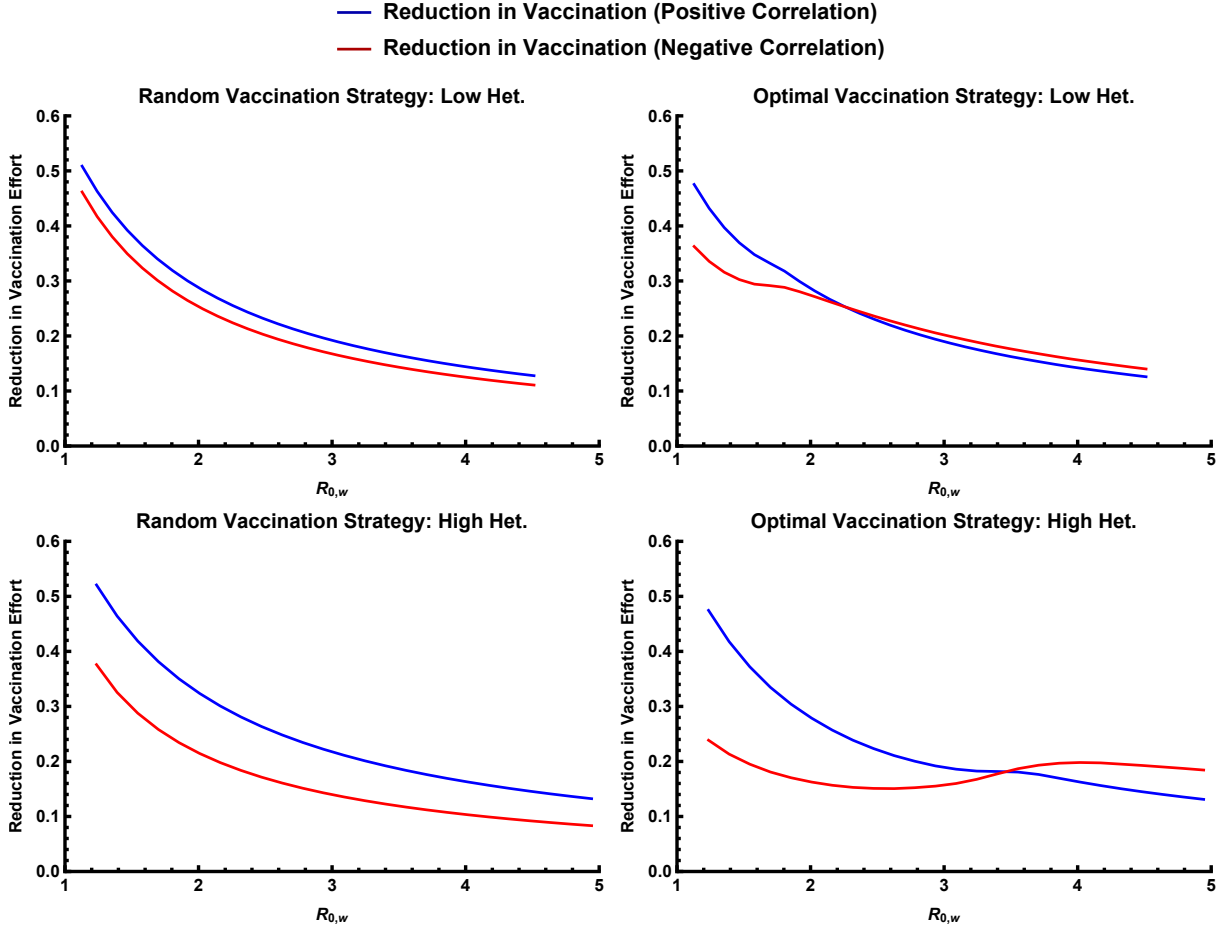


Figure 1.3: The fractional reduction in prophylaxis vaccination effort for both vaccine designs and strategies. We hold the vaccine  $R_0$  constant, and proportionally increase the pathogen transmission parameters, allowing us to look at a range of global  $R_{0,w}$  values. Parameter values are as followed: (Top panels) Vaccine transmission positive correlation:  $R_{0,v,1,1}=0.45$ ,  $R_{0,v,2,2}=0.27$ ,  $R_{0,v,1,2}=0.18$ ,  $R_{0,v,2,1}=0.18$ , Vaccine transmission negative correlation:  $R_{0,v,1,1}=0.27$ ,  $R_{0,v,2,2}=0.45$ ,  $R_{0,v,1,2}=0.18$ ,  $R_{0,v,2,1}=0.18$ , Pathogen transmission:  $R_{0,w,1,1}=\text{range}(0.91-3.63)$ ,  $R_{0,w,2,2}=\text{range}(0.54-2.17)$ ,  $R_{0,w,1,2}=\text{range}(0.36-1.44)$ ,  $R_{0,w,2,1}=\text{range}(0.36-1.44)$ . (Bottom panels) Vaccine transmission positive correlation:  $R_{0,v,1,1}=0.54$ ,  $R_{0,v,2,2}=0.18$ ,  $R_{0,v,1,2}=0.18$ ,  $R_{0,v,2,1}=0.18$ , Vaccine transmission negative correlation:  $R_{0,v,1,1}=0.18$ ,  $R_{0,v,2,2}=0.54$ ,  $R_{0,v,1,2}=0.18$ ,  $R_{0,v,2,1}=0.18$ , Pathogen transmission:  $R_{0,w,1,1}=\text{range}(1.09-4.35)$ ,  $R_{0,w,2,2}=\text{range}(0.36-1.45)$ ,  $R_{0,w,1,2}=\text{range}(0.36-1.44)$ ,  $R_{0,w,2,1}=\text{range}(0.36-1.44)$ . Parameters conserved across panels:  $\gamma=0.02$ ,  $d=0.01$ ,  $b_1=10$ ,  $b_2=10$ .

In cases where it is feasible to deliver vaccines to subgroups optimally, vaccines that mimic the pathogen's patterns of transmission (positively correlated) are no longer guaranteed to be the best option. Specifically, if the local pathogen  $R_0$  is greater than unity

in only one subgroup, a positively correlated vaccine continues to be the best option. If, on the other hand, the local pathogen  $R_0$  is greater than unity in both populations, a negatively correlated vaccine can become the most beneficial vaccine design (a specific example being Figure 1.2). This reversal occurs because vaccination targets the subgroup of the population with highest pathogen transmission, reducing the susceptible population in that subgroup and effectively limiting the potential for vaccine transmission. Consequently, a vaccine with patterns of transmission negatively correlated with those of the pathogen spreads to a greater extent in the non-targeted subgroup, which in this case is the subgroup of the population that transmits the pathogen to a lesser degree. As a consequence, when both subgroups have local pathogen  $R_0$  values greater than unity, a negatively correlated vaccine benefits an optimal vaccination strategy by spreading well in the subgroup that is less targeted by direct vaccination.

#### 1.4.1 ENDEMIC PATHOGEN REDUCTION

If the pathogen is already endemic in a wildlife population and eradication is impossible, a transmissible vaccine may still be an effective tool for reducing pathogen incidence [8]. In this context, we use the proportional reduction in pathogen incidence relative to a non-transmissible vaccine to gauge the effectiveness of a transmissible vaccine (Appendix: Endemic pathogen reduction). Figure 1.4 shows the reduction in pathogen incidence across different levels of bias in vaccine distribution, defined as  $\delta_\sigma = \sigma_1 - \sigma_2$ . Our results show that a positively correlated vaccine generally outperforms a negatively correlated vaccine. Once more, when vaccination is random ( $\delta_\sigma = 0$ ), the benefit of a positive vaccine design remains relatively constant as population heterogeneity increases. In contrast, the effectiveness of the negatively correlated vaccine decreases with increasing heterogeneity (Figure 1.4).

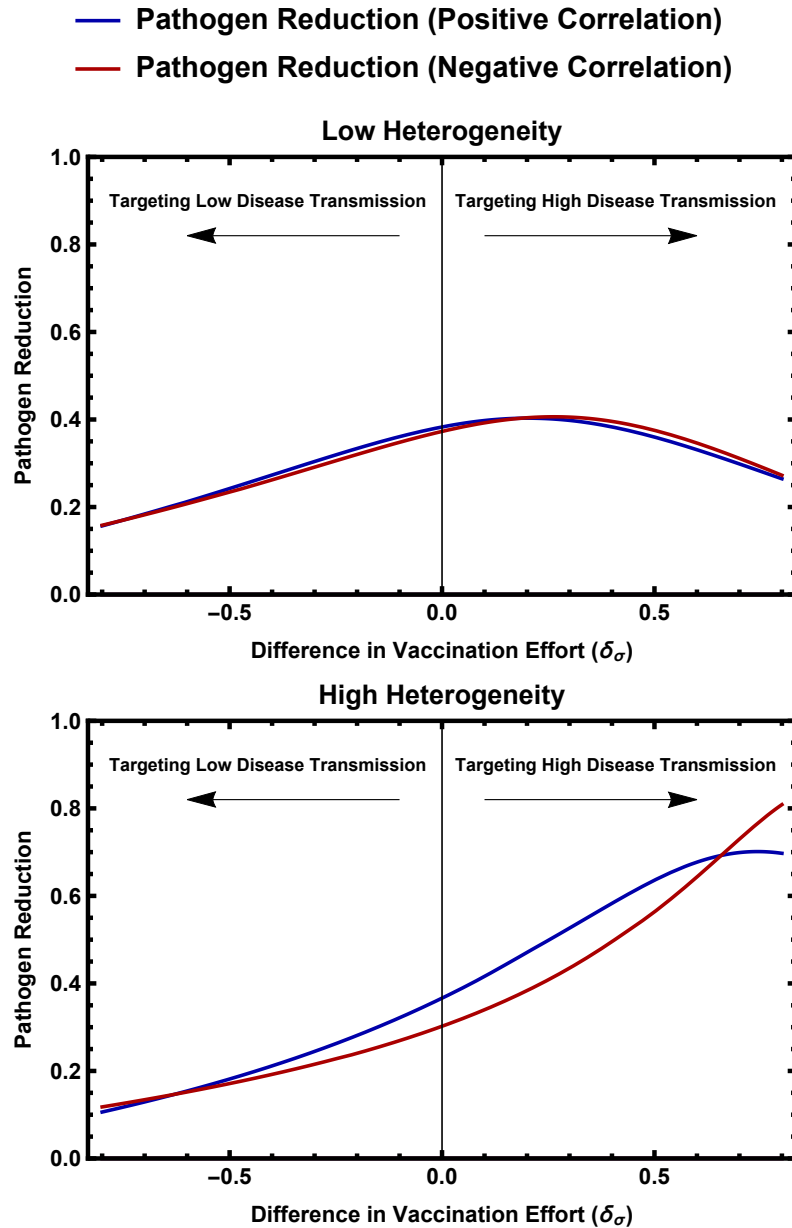


Figure 1.4: The proportional reduction in pathogen incidence attributed to vaccine transmission for a vaccine experiencing negative and positive correlation with respect to heterogeneity in pathogen transmission. Top panel: Global  $R_{0,w} = 3.70$ , global  $R_{0,v} = .88$ . Bottom panel: Global  $R_{0,w} = 4.19$ , global  $R_{0,v} = 1.00$ . Note that although the average within subgroup transmission remains constant, increasing heterogeneity increases the  $R_0$  of the infectious agents. Parameter values used in the figure: (Top panel) Vaccine transmission w/ positive correlation:  $R_{0,v,1,1}=0.7$ ,  $R_{0,v,2,2}=0.5$ , Vaccine transmission w/ negative correlation:  $R_{0,v,1,1}=0.5$ ,  $R_{0,v,2,2}=0.7$ , Pathogen transmission:  $R_{0,w,1,1}=2.94$ ,  $R_{0,w,2,2}=2.1$ . (Bottom Panel) Vaccine transmission w/ positive correlation:  $R_{0,v,1,1}=0.9$ ,  $R_{0,v,2,2}=0.3$ , Vaccine transmission w/ negative correlation:  $R_{0,v,1,1}=0.3$ ,  $R_{0,v,2,2}=0.9$ , Pathogen transmission:  $R_{0,w,1,1}=3.78$ ,  $R_{0,w,2,2}=1.26$ . Parameters conserved across panels:  $\bar{\sigma}=0.4$ ,  $\gamma=0.02$ ,  $d=0.01$ ,  $b_1=10$ ,  $b_2=10$ ,  $R_{0,v,1,2}=0.26$ ,  $R_{0,v,2,1}=0.26$ ,  $R_{0,w,1,2}=1.1$ ,  $R_{0,w,2,1}=1.1$ .

If the subgroup of the population that transmits the pathogen to a greater degree is preferentially targeted, the benefit of a transmissible vaccine increases with population heterogeneity, and the optimal vaccination strategy becomes more biased towards the subgroup that transmits the pathogen to a high degree (right side of Figure 1.4). Similar to the prophylaxis result, if the optimal vaccination strategy can be achieved and both population subgroups maintain an  $R_0$  greater than one, a negatively correlated transmissible vaccine is the most beneficial vaccine design. This result can be seen in Figure 1.4 where the two vaccine designs switch in order of benefit. However, if the subgroup of the population that weakly transmits the pathogen is preferentially targeted, the benefit of a transmissible vaccine is greatly diminished across a wide range of heterogeneity in host transmission (Figure 1.4). This occurs because when the pathogen is endemic, a high proportion of the high transmission subgroup is already infected with the pathogen, thus reducing vaccine transmission.

#### 1.4.2 SNV INVASION IN DEER MICE

Many viruses in wildlife populations, including Sin Nombre virus (SNV) in deer mice, maintain relatively low population level  $R_0$  values, typically estimated to be between one and two [18]. Even though these low  $R_0$  values suggest that disease control should be possible with relatively low vaccine coverage, the challenges of delivering a traditional vaccine to wildlife populations make meeting even these low thresholds a formidable challenge. To evaluate how a transmissible vaccine would perform in a situation where host access is limited, we consider SNV in deer mice, a virus in which transmission is mostly facilitated by males [19, 20].

When parameterized with data on SNV in deer mice, our model indicates that if a non-transmissible vaccine is used, a strongly biased vaccination strategy may be required to prevent pathogen invasion in a population of deer mice when vaccination effort is constrained (Appendix: SNV Invasion in Deer Mice, Figure 1.5)). However, biasing

vaccination effort towards male deer mice may be nearly impossible. In contrast, a transmissible vaccine can achieve prophylaxis over a much broader range of direct vaccination strategies (blue curves in Figure 1.5). In particular, a transmissible vaccine can prevent pathogen invasion, even when applied randomly to males and females, a much more realistic goal. We constrain the vaccination effort in this example to account for the inability to vaccinate most wildlife populations to a high degree. Although vaccination campaigns significantly differ based on the biological system of interest, we include reference to a rabies vaccination campaign to simply highlight the fact that a SNV vaccination campaign would be limited in some sense. Still, our results suggest a transmissible vaccination program (positive or negative correlation) could achieve population protection using a substantially reduced level of direct vaccination when compared to a traditional vaccine (Figure 1.5). Our analyses demonstrate that a transmissible vaccine could facilitate control of SNV for scenarios where vaccine and pathogen transmission correlate positively or negatively; however, the benefits of vaccine transmission are maximized when the correlation is positive. This occurs because SNV experiences a low population level  $R_{0,w}$ , where the pathogen only circulates well in one of the population subgroups (here defined as males).

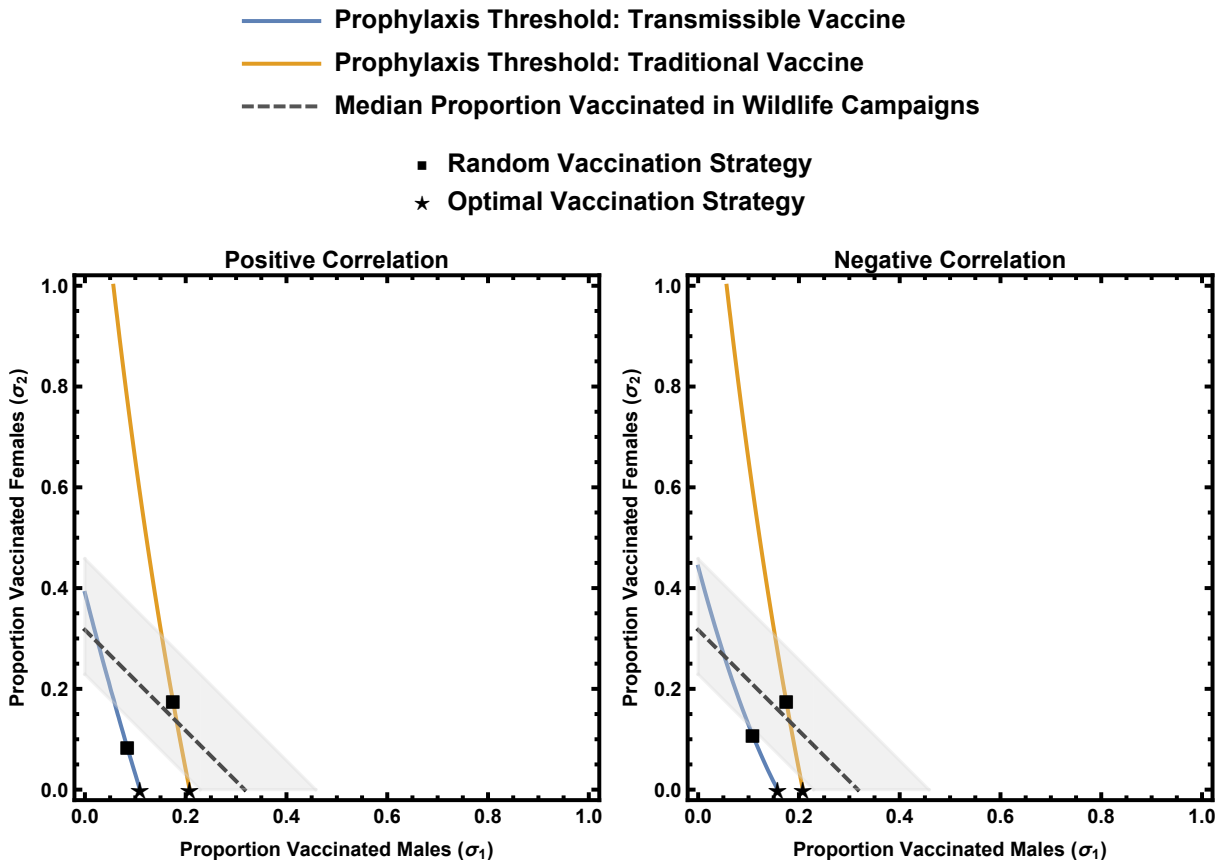


Figure 1.5: Proportion of male/female deer mice that must be vaccinated for prophylaxis against Sin Nombre Virus. The pathogen maintains a global  $R_{0,w} = 1.21$ , and two possible vaccine designs maintaining a global  $R_{0,v} = 0.61$ . The gray region provides a reference for typical values of the proportion of individuals successfully vaccinated in a wildlife vaccination campaign (see Appendix: SNV Invasion in Deer Mice). Fractional reduction in vaccination effort provided by a transmissible vaccine (left to right): a.) Optimal strategy=0.47, Random strategy=0.52, b.) Optimal strategy=0.24, Random strategy=0.38. Parameters: a.)  $R_{0,v,1,1}=0.53$ ,  $R_{0,v,2,2}=0.18$ ,  $R_{0,v,1,2}=0.18$ ,  $R_{0,v,2,1}=0.18$ ,  $R_{0,w,1,1}=1.06$ ,  $R_{0,w,2,2}=0.36$ ,  $R_{0,w,1,2}=0.36$ ,  $R_{0,w,2,1}=0.36$ , b.)  $R_{0,v,1,1}=0.18$ ,  $R_{0,v,2,2}=0.53$ ,  $R_{0,v,1,2}=0.18$ ,  $R_{0,v,2,1}=0.18$ ,  $R_{0,w,1,1}=1.06$ ,  $R_{0,w,2,2}=0.36$ ,  $R_{0,w,1,2}=0.36$ ,  $R_{0,w,2,1}=0.36$ .

## 1.5 DISCUSSION

Our study demonstrates that transmissible vaccines may provide a useful tool for controlling zoonoses in heterogeneous wildlife populations. However, maximizing the potential benefit of a transmissible vaccine requires careful consideration of the structure of the target population, the transmission characteristics of the pathogen and vaccine,

and the extent to which the vaccine can be preferentially administered to subgroups. For instance, if the target pathogen is characterized by self-sustained spread in only one subgroup of the population, a transmissible vaccine with transmission coefficients positively correlated with those of the pathogen is the best option. We have shown this to be the case for a population of deer mice, where the pathogen maintains an  $R_0$  greater than one in only the males (see Appendix: SNV Invasion in Deer Mice). Since many pathogens in wildlife populations have relatively low  $R_0$  values [18], this suggests that the optimal transmissible vaccine will generally be one designed to mirror the transmission patterns of the target pathogen. If, however, the subgroups of the target population maintain local  $R_0$  values greater than one, there are scenarios where it would be best to design a transmissible vaccine with patterns of transmission opposite to those of the pathogen.

Including heterogeneity in host transmission in epidemiological models generally inflates the global  $R_0$  of an infectious agent [15]. Therefore, intuition suggests that a transmissible vaccine would benefit from heterogeneity in host transmission because the vaccine would spread through high transmission pathways in the population, effectively vaccinating more susceptible individuals than in a population with homogeneous transmission. Indeed, this intuition holds for another transmissible therapy known as TIPs, where high transmission individuals are autonomously targeted in the population [13]. However, we have demonstrated that this result does not hold for a weakly transmissible vaccine targeting pathogens that are already present in the population. The reason for this stems from differences in the biology of the transmissible therapies. TIPs maintain the ability to autonomously target high transmission individuals because TIP transmission is facilitated by co-infection with the targeted pathogen. Conversely, a transmissible vaccine competes with the wild-type pathogen for susceptible hosts. Therefore, the realized boost in  $R_0$  that a transmissible vaccine experiences from host heterogeneity is neutralized by a proportional boost in the pathogen  $R_0$ .

Although our model yields insights into the performance of transmissible vaccines in



heterogeneous populations, it could be extended in numerous ways. For instance, our model assumes that vaccination can target only susceptible individuals, whereas wildlife vaccination programs often rely on distributing vaccine laced baits that target only those individuals who actively forage. Additionally, our model assumes that recovery rates from vaccine and pathogen infection are equal. This may be a reasonable assumption for an attenuated transmissible vaccine, but may not hold for an engineered recombinant vector vaccine [17]. Generalizing our model to these alternative scenarios is an important focus for future work, particularly as parameter estimates become available for transmissible vaccines now under development [7, 21].

Upon further development of transmissible vaccines, we will gain better insight into the manufacturing process, and the cost to produce such vaccines. If transmissible vaccines can be produced at a comparable cost to traditional vaccines, however, they will greatly reduce the cost of a wildlife vaccination campaigns. Our model analyses demonstrate this point by showing how vaccine transmission between individuals can greatly reduce the threshold vaccination rate required for prophylaxis or a desired level of pathogen reduction. Even if transmissible vaccines cost more than traditional vaccines, our models suggest they may still be more cost effective, although this will depend largely on the epidemiological details of the target pathogen and the transmission rate of the transmissible vaccine.

## 1.6 CONCLUSION

Although a transmissible vaccine does not receive a significant boost in performance due to host heterogeneity, our analyses indicate that they can still be an effective tool for reducing pathogen prevalence and preventing pathogen invasion in wildlife populations. Our models indicate that vaccine transmission significantly reduces the threshold of vaccination effort required to prevent pathogen spread in heterogeneous wildlife populations. When these thresholds cannot be met, vaccine transmission greatly reduces pathogen

prevalence in a heterogeneous population. Together, our analyses provide support for the continued development of transmissible vaccines to control zoonoses in wildlife reservoirs.

## 1.7 APPENDIX

This section elaborates on the methods used to evaluate the benefit of a transmissible vaccine in a population with heterogeneity in transmission. First, we find the level of direct vaccination required to prevent pathogen invasion, and use the resulting expression to define a benefit of vaccine transmission. Next, we analyze the case where pathogen invasion cannot be prevented, and instead evaluate a transmissible vaccine's ability to reduce a pathogen's prevalence in the host population. Finally, we parameterize our model to Sin Nombre virus in Deer mice, a wildlife system that has been documented to experience heterogeneity in transmission, to assess the effectiveness of a transmissible vaccine in a real-world scenario. As described by section 1.3 in the main text, we developed a system of differential equations to describe the population dynamics of a transmissible vaccine in a heterogeneous population:

$$\begin{aligned}
 \frac{dS_i}{dt} &= b_i(1 - \sigma_i) - dS_i - \sum_{j=1}^2 (\beta_{v,i,j}S_iV_j + \beta_{w,i,j}S_iW_j) \\
 \frac{dV_i}{dt} &= b_i\sigma_i - (\gamma + d)V_i + \sum_{j=1}^2 \beta_{v,i,j}S_iV_j \\
 \frac{dW_i}{dt} &= -(\gamma + d)W_i + \sum_{j=1}^2 \beta_{w,i,j}S_iW_j \\
 \frac{dR}{dt} &= -dR + \sum_{j=1}^2 (\gamma V_j + \gamma W_j)
 \end{aligned} \tag{1.1}$$

We first non-dimensionalize equations (1.1) to reduce the number of parameters. We scale each state variable by the steady state carrying capacity of the corresponding subgroup,  $\frac{b_i}{d}$ , so that  $s_i = S_i/(\frac{b_i}{d})$ ,  $v_i = V_i/(\frac{b_i}{d})$ , and  $w_i = W_i/(\frac{b_i}{d})$ . We introduce non-dimensional basic reproduction numbers that describe the spread of the pathogen and

vaccine between each pair of population subgroups;  $R_{0,w,i,j} = \frac{\beta_{w,i,j}b_j}{d(d+\gamma)}$  describes the average number of secondary infections in subgroup  $i$  caused by an infected individual dropped into subgroup  $j$ . We also define a new non-dimensional parameter  $\hat{d} = \frac{d}{d+\gamma}$  that gives the probability of death before recovery of an infected individual. Substituting these new parameters and state variables into equations (1.1) yields the non-dimensionalized system:

$$\begin{aligned}\frac{ds_i}{dt} &= \hat{d}(1 - s_i - \sigma_i) - \sum_{j=1}^2 R_{0,w,i,j} s_i w_j - \sum_{j=1}^2 R_{0,v,i,j} s_i v_j \\ \frac{dw_i}{dt} &= -w_i + \sum_{j=1}^2 R_{0,w,i,j} s_i w_j \\ \frac{dv_i}{dt} &= -v_i + \hat{d}\sigma_i + \sum_{j=1}^2 R_{0,v,i,j} s_i v_j\end{aligned}\tag{1.2}$$

### 1.7.1 PATHOGEN PROPHYLAXIS

Preemptively vaccinating wildlife populations prior to the introduction of a pathogen threat can prevent the pathogen's invasion into the population and therefore reduce the chance of spillover into human populations [7]. To assess the utility of a transmissible vaccine in preventing pathogen invasion into a wildlife population, we first identify the vaccination thresholds required to prevent pathogen invasion for both a traditional and transmissible vaccine. We identify two relevant vaccination strategies, and then measure the benefit provided by vaccine transmission under each strategy. The first strategy, random vaccination, describes a scenario where vaccines are distributed evenly between subgroups so that  $\sigma_1 = \sigma_2 = \sigma$ . The second vaccine distribution strategy, optimal vaccination, describes a scenario where the vaccine can be preferentially disseminated to the subgroups in a way that minimizes the total vaccine distribution rate  $\hat{d}(\sigma_1 + \sigma_2)$  across all possible vaccination strategies along the prophylaxis threshold. For both vaccination strategies and for each parameter set, we define the benefit of vaccine transmission ( $B$ ), as the proportional reduction in the total vaccine distribution rate that results from a

transmissible vaccine:

$$B = \left( 1 - \frac{\sigma_{TV}}{\sigma_{NTV}} \right) \quad (1.3)$$

Here,  $\sigma_{TV}$  is the prophylaxis vaccination effort when using a transmissible vaccine, and  $\sigma_{NTV}$  is the prophylaxis vaccination effort when using a non-transmissible vaccine.

To derive vaccination thresholds that prevent pathogen invasion, we calculate the pathogen's global basic reproductive number  $R_{0,w}$  using the Next Generation Matrix (NGM) method [22]. Briefly, the NGM is a matrix whose elements describe the number of new infections of each type that are produced by each type of infected individual. The  $R_{0,w}$  is calculated as the spectral radius of the NGM. In equations (1.2), the infectious subsystem is

$$\begin{aligned} \frac{dw_1}{dt} &= -w_1 + R_{0,w,1,1}s_1w_1 + R_{0,w,1,2}s_1w_2 \\ \frac{dw_2}{dt} &= -w_2 + R_{0,w,2,1}s_2w_1 + R_{0,w,2,2}s_2w_2. \end{aligned} \quad (1.4)$$

We linearize around the steady-state that describes the vaccinated host population in the absence of the pathogen. Defining the perturbation from steady state as  $\tilde{w} = (\tilde{w}_1, \tilde{w}_2)$ , the linearized subsystem can be written in matrix form,

$$\dot{\tilde{w}} = J\tilde{w} \quad (1.5)$$

where,  $J$  is the  $2 \times 2$  Jacobian of the infectious subsystem (1.4) evaluated at the relevant pathogen-free equilibrium:

$$J = \begin{bmatrix} R_{0,w,1,1}s_1^* - 1 & R_{0,w,1,2}s_1^* \\ R_{0,w,2,1}s_2^* & R_{0,w,2,2}s_2^* - 1 \end{bmatrix}. \quad (1.6)$$

Next, we decompose the matrix components of  $J$  as the sum of two matrices,  $J = T_w + \Sigma_w$ . Here  $T_w$  contains terms from  $J$  that describe the production of new infected

individuals within each subgroup:

$$T_w = \begin{bmatrix} s_1^* R_{0,w,1,1} & s_1^* R_{0,w,1,2} \\ s_2^* R_{0,w,2,1} & s_2^* R_{0,w,2,2} \end{bmatrix}. \quad (1.7)$$

Specifically, element  $(i, j)$  of  $T_w$  describes the rate at which new infected hosts in subgroup  $i$  arise due to pathogen-infected individuals in subgroup  $j$ . The matrix  $\Sigma_w$  describes the rates at which hosts leave each infectious state, due to either death or recovery:

$$\Sigma_w = \begin{bmatrix} -1 & 0 \\ 0 & -1 \end{bmatrix}. \quad (1.8)$$

From  $T_w$  and  $\Sigma_w$ , the NGM with large domain is calculated as

$$\begin{aligned} K_L &= -\Sigma_w^{-1} \cdot T_w \\ &= \begin{bmatrix} s_1^* R_{0,w,1,1} & s_2^* R_{0,w,2,1} \\ s_1^* R_{0,w,1,2} & s_2^* R_{0,w,2,2} \end{bmatrix} \end{aligned} \quad (1.9)$$

Element  $(i, j)$  of  $K_L$  gives the number of secondary infections of type  $i$  that are produced by an individual of infectious type  $j$ , throughout the course of infection. The pathogen  $R_0$  is defined as the spectral radius of the NGM  $K_L$ :

$$R_{0,w} = \frac{1}{2} \left( \text{Tr}(K_L) + \sqrt{\text{Tr}(K_L)^2 - 4\text{Det}(K_L)} \right), \quad (1.10)$$

where  $\text{Tr}$  and  $\text{Det}$  denote the trace and determinant, respectively. Equation (1.10) gives the relationship between the number of susceptible individuals in each subgroup at the pathogen-free steady-state and the pathogen's ability to invade the population.

Prophylactic vaccination serves to reduce the steady state number of susceptible individuals  $s_1^*$  and  $s_2^*$ , and, if successful, reduces the pathogen's realized  $R_{0,w}$  to a value less than one. To evaluate the pathogen's  $R_0$  that results from a given direct vaccination effort,

we numerically solve for the steady states of equations (1.2) with the pathogen absent (i.e.  $w_1 = 0, w_2 = 0$ ). Specifically, we numerically integrate system (1.1) forward in time until the maximum magnitude of the differentials is less than  $10^{-4}$ . Numerical solutions were found using the `ParametricNDSolve` and `WhenEvent` functions in Mathematica version 10.4.1.0, and the Mathematica code is available as a supplementary file.

With this method, we determine the minimal amount of direct vaccination effort, given by  $\sigma_1 + \sigma_2$ , that reduces the pathogen's  $R_{0,w}$  to one for a non-transmissible vaccine. The benefit of vaccine transmission is measured as the fractional reduction in the amount of vaccination effort that is necessary to maintain the pathogen  $R_{0,w}$  at one (Equation (1.3)).

### 1.7.2 ENDEMIC PATHOGEN REDUCTION

If it is impossible to vaccinate the population to an extent that precludes pathogen invasion, the pathogen will invade and persist in the population. In this case, the benefit of vaccine transmission can be assessed by the reduction in the pathogen's incidence that can be attributed to vaccine transmission. Naturally, the reduction due to vaccine transmission will depend on how the vaccine is distributed to the subgroups of the population. To clarify the effect of biasing direct vaccination effort between the two subgroups, we reparameterized the model in terms of the average fraction of newborns vaccinated,  $\bar{\sigma} = \frac{1}{2}(\sigma_1 + \sigma_2)$ , for the two subgroups of the population. Additionally, we define  $\delta_\sigma = \sigma_1 - \sigma_2$ , as the bias toward subgroup 1 of the vaccination strategy. For a fixed average vaccination level, we vary  $\delta_\sigma$  to study how differentially targeting subgroups impacts the proportional reduction in pathogen incidence.

To calculate the reduction in pathogen incidence as a result of vaccine transmission, we numerically solve the system of differential equations (1.2) forward in time until steady state is reached, across a range of parameters that allow for pathogen persistence. We determine that the system has reached steady state once the maximum magnitude of the differentials is less than  $10^{-4}$ . Next, we calculate the total number of pathogen-

infected individuals in the aggregate population at steady-state that result when a non-transmissible vaccine is used, denoted  $w_0$ . We then calculate the incidence that results when a transmissible vaccine is used, termed  $w_{tv}$ . From these quantities, we calculate the proportional reduction  $P$  in pathogen incidence, as a result of vaccine transmission:

$$P = \left(1 - \frac{w_{tv}}{w_0}\right). \quad (1.11)$$

### 1.7.3 SNV INVASION IN DEER MICE

In this section, we parameterize our model to Sin Nombre virus (SNV), a type of Hantavirus that circulates in deer mice (*Peromyscus maniculatus*). When transmitted to human populations, SNV causes Hantavirus Pulmonary Syndrome (HPS), a deadly disease with a case fatality rate of about 40% [23, 24]. Studies on SNV prevalence in deer mice show that the pathogen spreads between males and females at different rates, resulting in a higher prevalence among males than females [20]. It is hypothesized that this heterogeneity in prevalence is maintained by aggressive interactions between males that, in turn, facilitate pathogen transmission [19].

Due to the high mortality rate caused by SNV in human populations [24], non-transmissible vaccines that target SNV in deer mice have been developed and tested [25, 26]; however, a widespread vaccination campaign has not yet been implemented. Here, we parameterize equations (1.2) to describe SNV transmission in an uninfected deer mouse population, and as before, quantify the benefit of using a transmissible vaccine to prevent the invasion of SNV. Here, the subgroups of our model allow us to track SNV infection among male (subgroup 1) and female (subgroup 2) deer mice. We use data on SNV prevalence in male and female deer mice, as reported in Adler, Clay, & Lehmer (2008), to parameterize a version of equations (1.2) that is specific to SNV when the vaccine is absent in the population. Because SNV infection is known to persist for the lifespan of deer mice [27], we set the recovery rate  $\gamma = 0$ , which, in the non-dimensional

model is equivalent to setting  $\hat{d} = 1$ . The resulting equations describing the susceptible and infectious classes for each subgroup,  $s_i$  and  $w_i$  are:

$$\begin{aligned}
\frac{ds_1}{dt} &= 1 - s_1 - (R_{0,w,1,1}w_1 + R_{0,w,1,2}w_2) s_1 \\
\frac{ds_2}{dt} &= 1 - s_2 - (R_{0,w,2,1}w_1 + R_{0,w,2,2}w_2) s_2 \\
\frac{dw_1}{dt} &= (R_{0,w,1,1}s_1) w_1 + (R_{0,w,1,2}s_1)w_2 - w_1 \\
\frac{dw_2}{dt} &= (R_{0,w,2,1}s_2)w_1 + (R_{0,w,2,2}s_2)w_2 - w_2
\end{aligned} \tag{1.12}$$

When simulated to steady state, equations (1.12) predict the equilibrium prevalence of SNV in male and female deer mice as a function of the four non-dimensional parameters  $R_{0,w,i,j}$ . We use this relationship to find values of  $R_{0,w,i,j}$  that produce similar prevalences of SNV in males and females reported in Adler, Clay, & Lehmer (2008). To further constrain the allowed values  $R_{0,w,i,j}$ , we assume that male-male interactions (interactions between hosts of subgroup 1) are responsible for most of the SNV transmission in the population. As a consequence,  $R_{0,w,1,1}$  is larger than  $R_{0,w,1,2}$ ,  $R_{0,w,2,1}$ , and  $R_{0,w,2,2}$ . In addition, we assume that the rate of male-to-female, female-to-male, and female-to-female interactions are the same so that  $R_{0,w,1,2} = R_{0,w,2,1} = R_{0,w,2,2}$ . With these assumptions, we adjust the remaining two free parameters to match prevalence reported in Adler, Clay, & Lehmer (2008) yielding  $R_{0,w,1,1} = 1.06$  and  $R_{0,w,1,2} = R_{0,w,2,1} = R_{0,w,2,2} = 0.36$ , resulting in predicted SNV prevalences of 0.19 (empirical: 0.19) in males, and 0.09 (empirical: 0.09) in females. To simplify the presentation of the terms  $R_{0,w,i,j}$ , we combine them into a matrix,  $R_{0,w}$ , defined as

$$R_{0,w} = \begin{pmatrix} 1.06 & 0.36 \\ 0.36 & 0.36 \end{pmatrix} \tag{1.13}$$

where entry  $(i, j)$  gives  $R_{0,w,i,j}$ .

The benefit of using a transmissible vaccine will clearly depend on the terms  $R_{0,v,i,j}$ . Because empirical research into transmissible vaccine designs is still in its infancy, it is



not possible to use empirical data to parameterize the spread of the vaccine in the model. Instead, we assume that the average number of secondary infections per vaccine-infected host is half the average number of secondary infections per pathogen-infected host. In the supplementary Mathematica file, we show that this condition also implies that the global  $R_0$  of the vaccine is half of the global  $R_0$  of the pathogen. In addition to constraining the average amount of vaccine transmission in the population, we must also describe how the vaccine transmits between the various subgroups. We investigate two plausible vaccine behaviors, termed positive and negative correlation, that describe how the vaccine spreads relative to the biased spread of the pathogen. Values of the vaccine transmission matrix were selected to represent the most extreme scenarios of positive and negative correlation with the pathogen transmission matrix. The vaccine with positive correlation transmits the most within the subgroup that also spreads the pathogen best, so that

$$R_{0,v+} = \begin{pmatrix} 0.53 & 0.18 \\ 0.18 & 0.18 \end{pmatrix}. \quad (1.14)$$

Alternatively, the vaccine might be negatively correlated so that the pathogen spreads best in the subgroup with the least amount of within-group pathogen transmission, so that

$$R_{0,v-} = \begin{pmatrix} 0.18 & 0.18 \\ 0.18 & 0.53 \end{pmatrix}. \quad (1.15)$$

In our invasion analysis of SNV in a deer mouse population, we include a reference vaccination threshold of  $(\sigma_1 + \sigma_2) = .317$ , which is the median proportion of vaccinated individuals for rabies vaccination programs led by the USDA across multiple states, animal species, and years [28–32]. In addition to the median threshold, we include a shaded region that includes the 25<sup>th</sup> and 75<sup>th</sup> percentile of the vaccination data. We emphasize that, although vaccines targeting SNV in deer mice have been developed [26], a wide spread vaccination campaign has not been implemented. We understand that this data may not

relate to vaccinating deer mice, and simply include this measure to show that wildlife vaccination campaigns are inherently limited in the fraction of individuals that can be vaccinated.

## CHAPTER 2: THE ZOOSES END GAME: QUANTIFYING THE EFFECTIVENESS OF BETAHERPESVIRUS-VECTORED TRANSMISSIBLE VACCINES

### 2.1 ABSTRACT

Transmissible vaccines have the potential to revolutionize how zoonotic pathogens are controlled within wildlife reservoirs. A key challenge that must be overcome is identifying viral vectors that can rapidly spread immunity through a reservoir population. Because they are broadly distributed taxonomically, species specific, and stable to genetic manipulation, betaherpesviruses are leading candidates for use as transmissible vaccine vectors. Here we evaluate the likely effectiveness of betaherpesvirus vectored transmissible vaccines by developing and parameterizing a mathematical model using data from captive and free-living mouse populations infected with murine cytomegalovirus (MCMV). Forward simulations of our parameterized model demonstrate rapid and effective control for a range of pathogens, with pathogen elimination frequently occurring within a year of vaccine introduction. Our results also suggest, however, that the effectiveness of transmissible vaccines may vary across reservoir populations and with respect to the specific vector strain used to construct the vaccine.

### 2.2 INTRODUCTION

Pathogen transmission at the human-wildlife interface is a fundamental threat to human health. Examples of the detrimental effects that zoonotic spillover has on humans include the coronavirus (SARS-CoV-2) pandemic [33], the 2014-2015 Ebola virus epidemic [3], and the persistent threat of Lassa virus in West Africa [34, 35]. These spillover events illustrate the significant burden that zoonotic pathogens can impose on human populations and emphasize the importance of controlling zoonotic pathogens before spillover occurs.

Historically, mass vaccination and culling have been the two most prominent methods for controlling zoonotic pathogens within wildlife reservoirs. However, the success of these traditional control measures relies on the ability to vaccinate or remove a high proportion of the target animal population, a requirement that may often be infeasible [4, 36]. As a consequence, wildlife vaccination has generally proven successful at limiting spillover only in special cases where mass-distribution of vaccine-laced baits can be regularly accomplished (e.g., rabies carried by raccoons and foxes in North America and Europe, respectively) [37]. A novel approach that could overcome the challenges faced by traditional wildlife vaccination programs is to use recombinant vector vaccines capable of self-dissemination [7, 38]. Transmissible recombinant vector vaccines are constructed by engineering a benign vector virus to carry and express an immunogenic transgene from a specific target pathogen [17]. In theory, the resulting vaccine takes on the transmission characteristics of the vector virus, while triggering an immune response specific to the target pathogen. Leading candidates to serve as vectors for transmissible vaccines are the betaherpesviruses (e.g., murine cytomegalovirus (MCMV)) due to their broad taxonomic distribution, high species specificity, and mild or undetectable virulence in most natural reservoirs [39, 40].

Although previous modeling efforts have demonstrated the potential benefits of vaccine transmission [8, 41–45], these models have been general and not parameterized for specific candidate vaccine vectors or zoonotic pathogens. Further, existing models have focused almost exclusively on steady-state solutions and have not addressed the timescale over which zoonotic pathogens can be eliminated. Consequently, we do not yet know how well transmissible vaccines developed using betaherpesvirus vectors (such as MCMV) are likely to work in practice. To address this gap, we develop a mathematical model describing the spread of an MCMV-vectored transmissible vaccine through a reservoir population and parameterize it using data from captive and free-living mouse populations. We use this parameterized model to predict how rapidly MCMV-vectored transmissible vaccines

can eliminate pathogens with different properties and to quantify the scope for variable outcomes across reservoir populations and across vaccines developed from different vector strains.

## 2.3 RESULTS

### 2.3.1 PATHOGENS THAT GENERATE ACUTE VIRAL INFECTIONS ARE VULNERABLE TO TRANSMISSIBLE VACCINES

We used Approximate Bayesian Computation (ABC) to parameterize an epidemiological model tuned to the biology of betaherpesviruses such as MCMV. Our approach capitalized on a unique data set that tracked the spread of MCMV through naive mouse populations inhabiting semi-natural enclosures [46]. Applying our ABC algorithm to these time-series data allowed us to estimate the transmission rate of MCMV ( $\beta_v$ ) and the rate at which exposed individuals become infectious ( $\alpha_1$ ) as the mode of the bivariate posterior distribution (Figure 2.1). Next, we used these parameter estimates to predict how rapidly an MCMV-vectored transmissible vaccine could reduce pathogen prevalence. Specifically, simulating the interaction between transmissible vaccine and pathogen revealed that the time required to reduce pathogen prevalence by ninety-five percent varies widely across pathogens and depends on pathogen  $R_0$  and the pathogen's infectious period. For example, our model predicts an MCMV-vectored transmissible vaccine will reduce pathogen prevalence by 95% in 156 days if the pathogen has an  $R_0$  of 1.5 and infectious period of 10 days, but will require 1028 days to accomplish an identical reduction for a pathogen with an  $R_0$  of 2.5 and infectious period of 365 days (Figure 2.2).

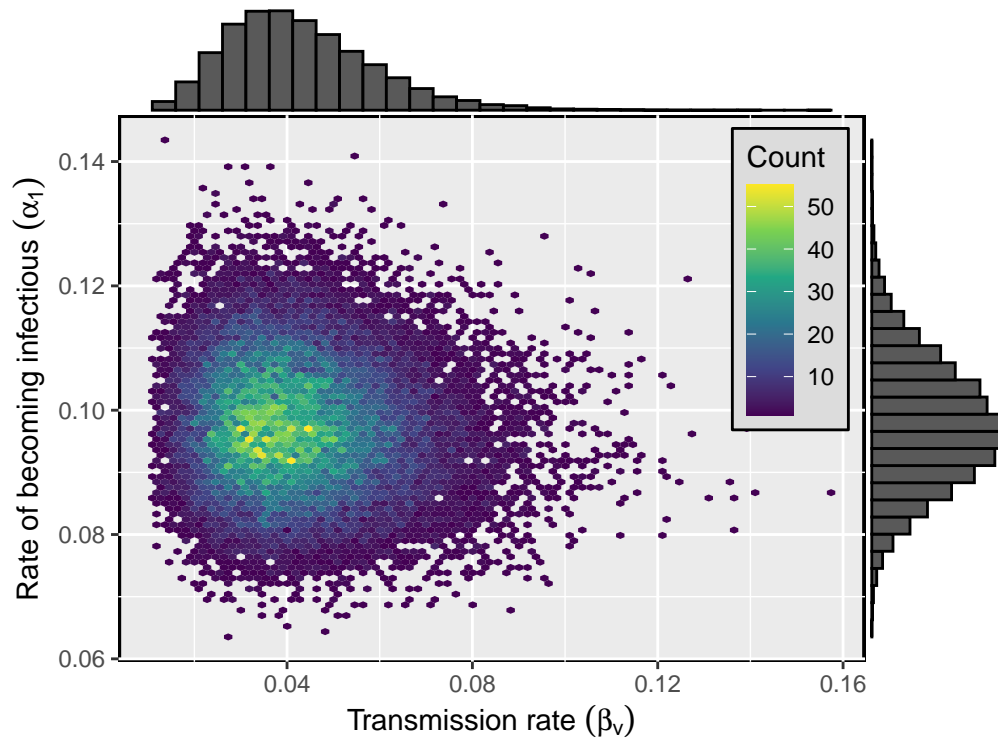


Figure 2.1: Bivariate posterior distribution of the transmission rate ( $\beta_v$ ) and the rate at which individuals exposed to the virus transition into the infectious class ( $\alpha_1$ ). The marginal distribution of the transmission rate and rate of becoming infectious are displayed on the top and right of the density plot, respectively. The modal values of the distribution are as followed:  $\beta_v = 0.033 \text{ individual}^{-1} \text{ day}^{-1}$ ,  $\alpha_1 = 0.099 \text{ day}^{-1}$ .

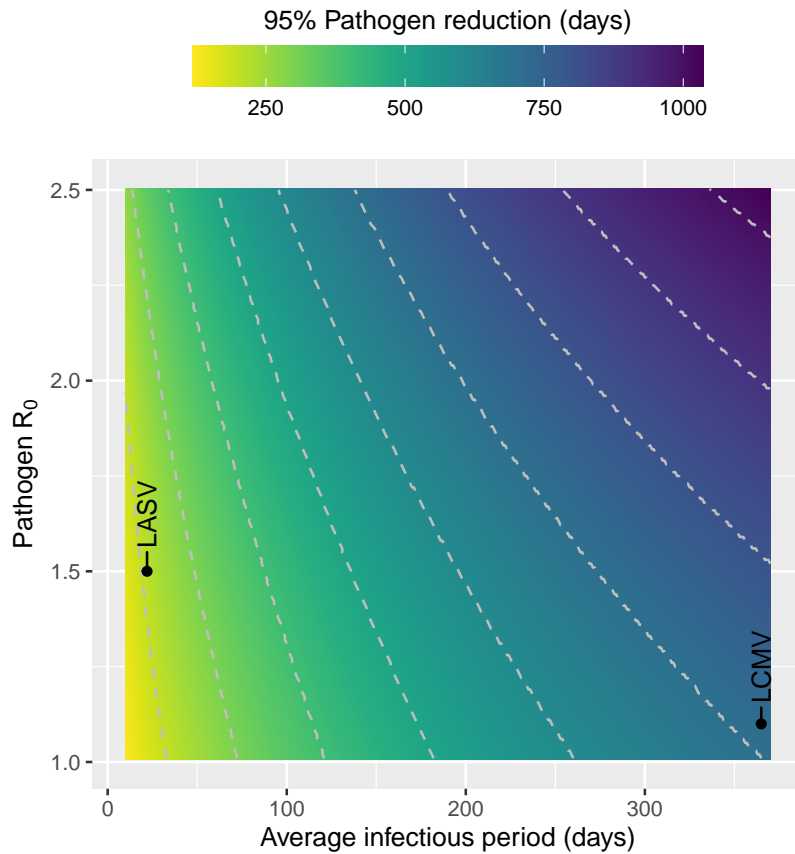


Figure 2.2: Time to ninety-five percent pathogen reduction as a function of pathogen  $R_0$  and the infectious period ( $1/\gamma$ ). Simulations start at the steady state quantities for susceptible and pathogen infected individuals, and 10% of the susceptible population is exposed to the transmissible vaccine. The pathogens highlighted in this figure include Lassa virus (LASV) and Lymphocytic Choriomeningitis virus (LCMV).

To better ground our predictions in the biology of specific pathogens, we used our model to predict the impact of an MCMV-vectored transmissible vaccine on Lassa virus (LASV) and lymphocytic choriomeningitis (LCMV). Both pathogens regularly spillover into the human population from rodent reservoirs and cause significant morbidity [47,48]. Although the primary reservoir of LASV, the multimammate rat *Mastomys natalensis*, is only distantly related to the domestic mouse, both LASV and LCMV do infect species within the genus *Mus* [49]. Using published estimates for seroprevalence and infectious period for these pathogens [50,51] we developed models describing their response to an

MCMV-vectored transmissible vaccine. Numerical analyses of these models suggest that LASV is very susceptible to control with an MCMV-vectored transmissible vaccine, with 95% reduction achieved in only 212 days. In contrast, our model predicts that LCMV is more recalcitrant and requires 716 days for 95% reduction to be achieved (Figure 2.2). The greater resistance to the vaccine exhibited by LCMV is largely explained by its increased infectious period which we have assumed is, on average, lifelong. In contrast, the infectious period for LASV has been estimated to be 22 days, on average [50, 51]. These results highlight that pathogens that generate acute, short-term infections and have relatively low  $R_0$  are most readily controlled using MCMV-vectored transmissible vaccines.

We further explored the uncertainty in our predictions for the impact of an MCMV-vectored transmissible vaccine by conducting simulated vaccination campaigns where the vaccine parameters were drawn at random from the bivariate posterior distribution (i.e., Figure 1). Performing 100 simulated vaccine releases for LASV and for LCMV revealed considerable uncertainty in the timescale over which each pathogen can be locally eliminated. Specifically, our results show that the time required for LASV to be reduced by 95% ranges from 121-371 days post-vaccine introduction, whereas the time required for LCMV to be reduced by 95% ranges from 609-940 days post-vaccine introduction (Figure 2.3).



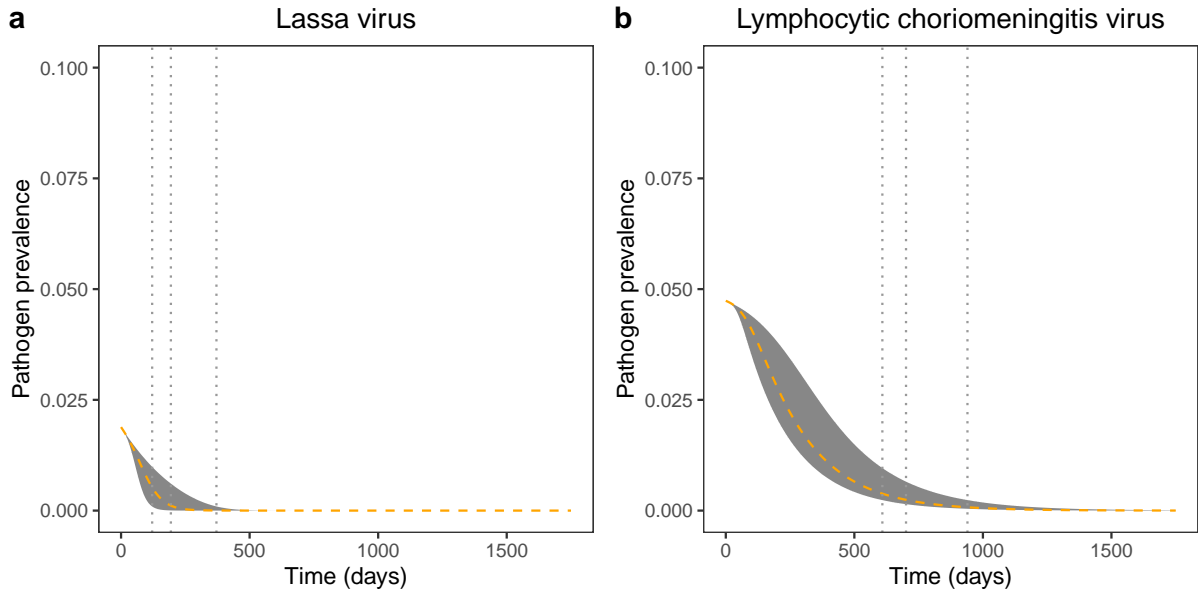


Figure 2.3: Temporal dynamics of (a) Lassa virus (LASV) and (b) Lymphocytic Choriomeningitis virus (LCMV) reduction as a result of using a MCMV-vectored transmissible vaccine. Simulations are initialized at the steady state quantities for susceptible and pathogen infected individuals, with 10% of the susceptible population removed and exposed to the transmissible vaccine. For each pathogen example we randomly sampled  $\beta_v$  and  $\alpha_1$  from the posterior distribution 100 times, and simulated our model forward in time for each set of parameters. The grey region represents the 100 simulations, where the orange dashed line is the mean. The grey vertical lines indicate the minimum, mean, and maximum time to 95% pathogen reduction ((a) min=121 days, mean=371 days, max=194 days (b) min=609 days, mean=701 days, max=940 days).

### 2.3.2 TRANSMISSIBLE VACCINES ARE ROBUST TO VARIATION IN EFFICACY

The preceding results are predicated on the development of an MCMV-vectored transmissible vaccine that blocks 100% of pathogen transmission. In reality, however, vaccine efficacy often varies in wild animal populations, as demonstrated by vaccination campaigns using oral rabies vaccine (SAG2) [52]. To account for imperfect vaccine efficacy, we extended our basic model to allow partial blocking of pathogen transmission (see Supplemental Information). With the extended model we explored how vaccine efficacy, quantified as the reduction in pathogen transmission rate in vaccinated animals ( $\rho$ ), im-

pacts a transmissible vaccine's ability to protect a reservoir population from pathogen invasion, and also how it impacts the timing required to effectively eliminate an endemic pathogen.

We began our analysis by deriving the critical vaccine efficacy that must be achieved for a transmissible vaccine to protect a reservoir population from pathogen invasion. Specifically, results derived in the Supplementary Information show that the efficacy of an MCMV-vectored transmissible vaccine must exceed the critical value:

$$\rho_{crit} = \frac{R_{0,v}}{R_{0,w}} \left( \frac{1 - R_{0,w}}{1 - R_{0,v}} \right). \quad (2.1)$$

to prevent the spread of a pathogen. Numerical analyses suggest this critical value also represents the vaccine efficacy required for a transmissible vaccine to eliminate an endemic pathogen. Without reintroduction of the vaccine, this result demonstrates that pathogen elimination requires that vaccine  $R_0$  exceed pathogen  $R_0$  by an amount that is inversely proportional to vaccine efficacy. Simply put, the lower vaccine efficacy, the more transmissible it must be to control a pathogen.

Although vaccine efficacy plays an important role in determining the success or failure of pathogen control, it has only a modest influence on the timescale over which pathogen control occurs. Specifically, numerical simulations of MCMV-vectored transmissible vaccines show that if vaccine efficacy exceeds the critical value for eliminating LASV and LCMV, the timescale over which pathogen elimination occurs is relatively insensitive to vaccine efficacy (Figure 2.4).

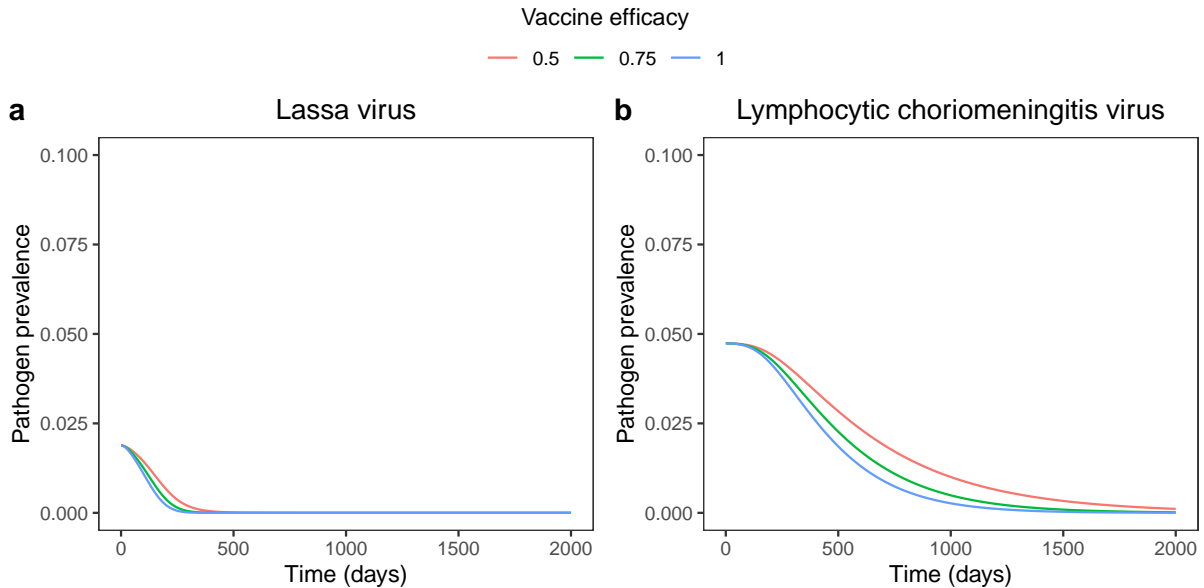


Figure 2.4: Temporal dynamics of (a) Lassa virus (LASV) and (b) Lymphocytic Choriomeningitis virus (LCMV) reduction as a result of using an MCMV-vectorized transmissible vaccine with varying levels of efficacy. Simulations are initialized at the steady state quantities for susceptible and pathogen infected individuals, where 10% of the susceptible population is removed and exposed to the transmissible vaccine.

### 2.3.3 RESERVOIR POPULATION AND VECTOR STRAIN MATTER

An additional source of uncertainty in our predictions arises from our reliance on data from MCMV introductions into naive, captive mouse populations using a single genetic variant of MCMV. Although the time-series data from these experimental introductions is invaluable for the opportunities it provides for robust parameter estimation, these parameters may vary across wild mouse populations and MCMV strains used as vaccine vectors. We explored the possible magnitude of this variation by analyzing published data describing the prevalence of two MCMV strains, as defined by the genotype of ie1, a major immunodominant T cell epitope [53, 54], within four populations of free-living wild mice [55]. Assuming the prevalence of these MCMV sequences represents their strain and population specific equilibrium, we can use classical epidemiological theory to predict the maximum  $R_0$  of a pathogen that could be eliminated by a transmissible vaccine

constructed from each MCMV strain within each reservoir population [56]. Specifically, we know that the fraction of a population that must be vaccinated to protect against a pathogen with  $R_0$  is equal to

$$p = 1 - \frac{1}{R_0}. \quad (2.2)$$

Rearranging equation (2.2) and substituting in the strain and location specific values of MCMV prevalence for  $p$  allows us to calculate the range of pathogen  $R_0$ 's that an MCMV-vectored transmissible vaccine with perfect efficacy could protect against (Table 2.1). The results of this simple analysis reveal considerable variation in the protective ability of transmissible vaccines constructed from different MCMV strains and used in different reservoir populations, with the range of pathogen  $R_0$  that can be suppressed ranging from 1.17 to 11.72. We extended this simple equilibrium analysis to the timescale of pathogen elimination by combining our ABC estimate for  $\alpha_1$  (section 2.5.2) with the prevalence of the MCMV variants within each of the four free-living mouse populations to yield estimates for the transmission rate of each MCMV strain within each reservoir population (Table 2.1).

Location	Strain	Pathogen Protection ( $R_0$ )	$\beta_v$ Estimate	Method	Data Source
Outdoor Enclosure	N1	11.72	0.033	ABC	[46]
Boullanger Island	G4	1.29	0.0036	Steady State	[55]
Macquarie Island	G4	11.35	0.032	Steady State	[55]
Canberra	G4	1.75	0.0049	Steady State	[55]
Walpeup	G4	1.69	0.0048	Steady State	[55]
Boullanger Island	K181	7.83	0.022	Steady State	[55]
Macquarie Island	K181	1.17	0.0033	Steady State	[55]
Canberra	K181	2.60	0.0073	Steady State	[55]
Walpeup	K181	1.62	0.0046	Steady State	[55]

Table 2.1: MCMV parameter estimates found using a combination of Approximate Bayesian Computation and steady-state methods. It is important to note that the N1 strain was not found in any of the natural populations that were sampled across Australia, therefore our only N1 sample comes from the enclosure study. Further, to account for possible sampling error during the capture of rodents, we calculated the Clopper–Pearson 95% confidence interval on the MCMV sampling data, and then calculated the  $\beta_v$  estimate. To be conservative in our parameter estimate, we used the minimum value from the confidence interval.

Our results reveal potentially important spatial variation in the time required for a transmissible vaccine to reduce pathogen prevalence by ninety-five percent. For example, the prevalence of a pathogen with an  $R_0 = 2$  is reduced by ninety-five percent in only three of the four locations (Figure 2.5, right panel). Even in the three locations where a ninety-five percent reduction is achieved, the time it takes to reach this objective differs by thousands of days between the three locations and the two MCMV strains defined by their *ie1* genotype.

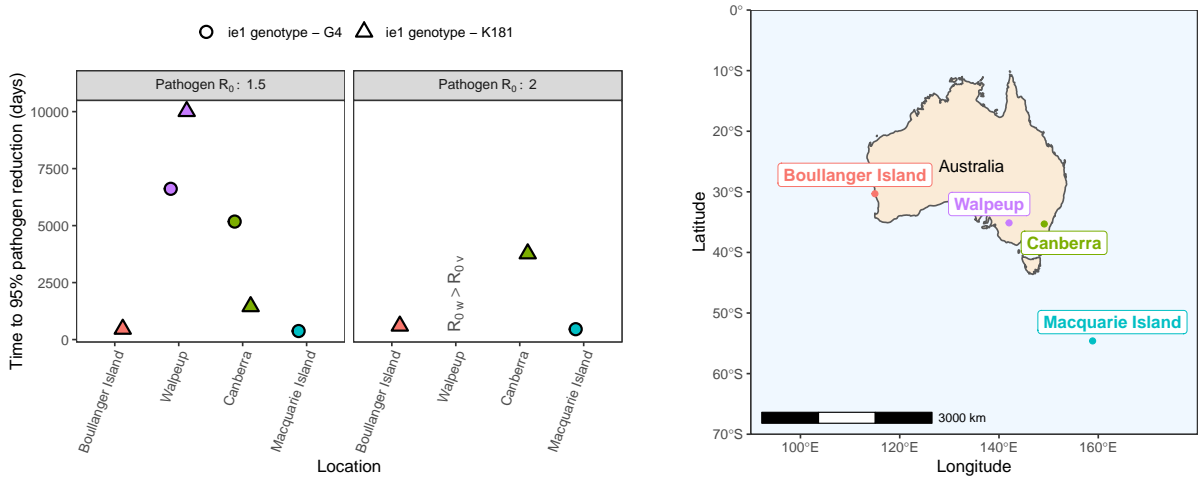


Figure 2.5: (a) Time to ninety-five percent pathogen reduction across four geographic locations. Simulations start at the steady state quantities for susceptible and pathogen infected individuals (see Supplementary Information), where 10% of the susceptible population is removed and exposed to the transmissible vaccine.  $R_{0,w} > R_{0,v}$  represents the scenario when the vaccine fails to reduce the pathogen. (b) Geographic locations represented in the data.

## 2.4 DISCUSSION

We have developed the first parameterized model predicting how much, and how rapidly, a betaherpesvirus-vectored transmissible vaccine can be expected to reduce the prevalence of a target pathogen. Our results demonstrate that the most vulnerable pathogens are those with relatively short infectious periods and a modest  $R_0$ . Pathogens that maintain a greater  $R_0$ , or that generate long-term chronic infections take longer to eliminate or, in some extreme cases, may be impervious to betaherpesvirus-vectored

transmissible vaccines altogether. Further, our results demonstrate that MCMV-vectored transmissible vaccines remain effective against a broad range of pathogens even when they provide less than perfect blocking of pathogen transmission. Perhaps most importantly, however, our results suggest that the effectiveness of MCMV-vectored transmissible vaccines may depend on the virus strain used to construct the vaccine and the target population into which the vaccine is ultimately deployed. If this prediction is borne out, it complicates the design of transmissible vaccines, and suggests it may be difficult to develop “universal” transmissible vaccines that transmit well across geographically distinct reservoir populations.

Although our results support betaherpesvirus-vectored transmissible vaccines as effective tools, these results are tempered by several important assumptions. First, and of critical importance, is our assumption that MCMV is capable of superinfection. This assumption is supported by studies showing that betaherpesviruses like MCMV can superinfect animals already infected with MCMV [55, 57]. At the same time, however, other studies have suggested superinfection is much more challenging [58–60] and may be achievable only by genetically differentiated MCMV strains. If superinfection requires genetic divergence, transmissible vaccines constructed from locally common betaherpesvirus strains or constructed in a way that results in the rapid loss of their immunogenic cargo, are unlikely to succeed [9, 42, 44]. Second, our inferences drawn from wild populations assume the geographic distribution of MCMV prevalence was at steady state and that differences in equilibrium prevalence reflect location specific transmission rates. There are, of course, many reasons this may not be true, including the possibility that geographic variation in MCMV prevalence is shaped by seasonal fluctuations in the population size of the target reservoir [61]. Third, we have assumed betaherpesvirus-vectored transmissible vaccines will transmit to the same degree as the wild-type virus vector. This may not be the case, as genetically engineering the vector virus to carry an immunogenic transgene may in fact alter the transmissibility of the self-disseminating vaccine [62].

A clear but unavoidable limitation of our work is our reliance on data from Australian populations of *Mus musculus* [46,55]. We focused on these populations due to the availability of unique experimental and field data sets that do not yet exist for other beta-herpesviruses and reservoir populations. The limitation, of course, is that our results may not generalize well to other geographic regions or rodent reservoir populations of greater concern for viral spillover. In addition, we have defined a strain based on a 126 base pair sequence of the *ie1* gene [55]. And whilst this is a dominant T cell epitope, there are other genes within MCMV that could be expected to modulate geographical penetrations. Unfortunately, data on the prevalence of beta-herpesviruses within natural populations of important reservoir species is extremely scarce [57] and experiments tracking the spread of beta-herpesviruses through important reservoir populations absent all together. Until these data become available, our results represent the most robust possible assessment of the future utility of beta-herpesviruses for transmissible vaccine design.

Recombinant vector transmissible vaccines show promise for revolutionizing how we mitigate the risk of zoonotic disease. Our results support the pursuit of beta-herpesviruses, such as MCMV, as vaccine vectors but also highlight critical assumptions about the dynamics of reinfection on which this optimistic outlook rests. Conclusive judgement on the utility of beta-herpesviruses as transmissible vaccine vectors will require more extensive study of the interactions between vector strain diversity and superinfection in the wild. Combining this information with the predictive framework developed here will help ensure that the first recombinant vector transmissible vaccines realize their promise.

## 2.5 METHODS

### 2.5.1 EPIDEMIOLOGICAL MODEL FOR MCMV

To evaluate the effectiveness of a MCMV-vectored transmissible vaccine, we rely on a susceptible-exposed-infectious model, similar to the one previously described by Arthur et al. (2009). In the model, individuals can belong to one of three classes: susceptible to the



vaccine ( $S$ ), exposed to the MCMV-vectored transmissible vaccine via rodent transmission ( $E_1$ ), and actively infectious with the MCMV-vectored transmissible vaccine ( $V$ ). We do not model a recovered or immune class because infection with MCMV is thought to be lifelong [39, 63]. Throughout, we assume that the total population size, denoted  $N$ , is constant. Individuals are introduced into the susceptible class through a constant birth rate denoted  $b$  and die at rate  $d$ . Further, individuals transition from the susceptible class to the vaccine exposed class based on frequency dependent transmission with transmission coefficient  $\beta_v$ , and transition from being exposed to being actively infectious at rate  $\alpha_1$ . The deterministic model is as follows:

$$\frac{dS}{dt} = b - \frac{\beta_v SV}{N} - dS \quad (2.3)$$

$$\frac{dE_1}{dt} = \frac{\beta_v SV}{N} - \alpha_1 E_1 - dE_1 \quad (2.4)$$

$$\frac{dV}{dt} = \alpha_1 E_1 - dV. \quad (2.5)$$

### 2.5.2 MCMV MODEL PARAMETERIZATION USING TIME-SERIES DATA

To parameterize the model of MCMV spread, we rely on a detailed time course study conducted by Farroway et al. (2002) that was later presented in Arthur et al. (2009) [46, 64]. Together, these studies detail the time course and spread of MCMV in semi-natural enclosures of naive house mice (*Mus musculus*). The studies detail the transmission of Murine cytomegalovirus within six outdoor enclosures at six time points (day 35, day 49, day 63, and day 84). Each enclosure consisted of twenty two individuals, where six individuals were initially inoculated with MCMV via IP injection, and sixteen individuals remained initially susceptible.

We used Approximate Bayesian Computation (ABC) to parameterize a stochastic version our epidemiological model (Supplementary Information) with the time-series data.

Mechanistically, ABC estimates a posterior distribution for model parameters by 1.) drawing parameters at random from prior distributions informed by previous studies; 2.) using the sampled parameters to simulate the model forward in time; and 3.) including the sampled parameters in the posterior distribution if the simulated data are sufficiently close to the real data [65, 66]. Repeating steps 1-3 a sufficient number of times and for an appropriate acceptance threshold results in a posterior probability distribution for the model's parameters. To determine whether a simulation was sufficiently close to the real data, we calculated the total sum of squares (TSS) for the predicted prevalence of MCMV for a given time point across all enclosures. We then averaged the TSS across all time points, and compared this value to our critical threshold. For this study, we settled on a critical threshold of 0.10, as this is when we began to see diminishing returns with respect to the model fit and the time to produce the model fit. We repeated steps 1-3 until the posterior distribution contained 25,000 parameter sets defining a multivariate probability distribution for the transmission rate ( $\beta_v$ ) and the rate of becoming infectious with MCMV ( $\alpha_1$ ). We used the mode of the multivariate distribution as the estimate for these parameters ( $\beta_v = 0.033 \text{ individual}^{-1} \text{ day}^{-1}$ ,  $\alpha_1 = 0.099 \text{ day}^{-1}$ ).

### 2.5.3 MODEL PARAMETERIZATION USING MCMV PREVALENCE AND STEADY STATE ASSUMPTIONS

Although the time-series data set described in section 2.5.2 is ideal for developing parameter estimates, its generality may be limited by focusing on only a single geographic location and strain of MCMV. To generalize our parameter estimates to other locations, we used published estimates of MCMV prevalence from four Australian locations and two MCMV strains defined by their ie1 genotype [55]. A total of 117 *Mus musculus* were live trapped and qPCR was utilized to identify the presence of the two MCMV strains. For our modeling purposes, we assume that all individuals positively identified by qPCR are in the infectious or exposed classes ( $V$ ,  $E_1$ ) and that only qPCR negative individuals are

in the susceptible class ( $S$ ). Further, we refer to the fraction of individuals that tested positive for a particular MCMV strain as  $p_i$ , where  $i$  is the genotype of ie1 (i.e., K181, G4). To account for possible sampling error when testing *Mus musculus*, we calculate the Clopper–Pearson 95% confidence interval [67] for the prevalence of MCMV at each geographic location.

We use the prevalence data from Gorman et al. (2006) to estimate a transmission rate for each geographic location and MCMV strain. We start by solving for the steady state solution of equations (2.3-2.5) when MCMV is endemic. We then re-write the susceptible steady state expression in terms of the fraction of susceptible individuals, and solve the resulting expression for the transmission rate,  $\beta_v$ . The result is as follows:

$$\beta_v = \frac{d(d + \alpha_1)}{(1 - p_i)\alpha_1}. \quad (2.6)$$

Obtaining a numerical value for  $\beta_v$  requires knowledge of  $\alpha_1$  and  $d$ . We use the  $\alpha_1$  value derived in the ABC fitting process, and we choose  $d = 0.0027 \text{ day}^{-1}$  to describe an average lifespan of 365 days, typical of free-living *Mus musculus* [68].

#### 2.5.4 PREDICTING TIME TO NINETY-FIVE PERCENT PATHOGEN

##### REDUCTION

To explore a transmissible vaccine’s ability to reduce a pathogen, we extend the model of MCMV spread described in section 2.5.1 to include a target pathogen. In the extended model,  $W$  is a state variable that describes the number of hosts that are infected with the pathogen. Individuals that have been infected by the pathogen transmit at a frequency dependent rate  $\beta_w$ . Further, individuals recover from the pathogen at rate  $\gamma$ , and remain

in the recovered class ( $R$ ) for the remainder of their lives. The full model is as follows,

$$\frac{dS}{dt} = b - \frac{\beta_v SV}{N} - \frac{\beta_w SW}{N} - dS \quad (2.7)$$

$$\frac{dE_1}{dt} = \frac{\beta_v SV}{N} - \alpha_1 E_1 - dE_1 \quad (2.8)$$

$$\frac{dV}{dt} = \alpha_1 E_1 - dV \quad (2.9)$$

$$\frac{dW}{dt} = \frac{\beta_w SW}{N} - \gamma W - dW \quad (2.10)$$

$$\frac{dR}{dt} = \gamma W - dR. \quad (2.11)$$

To calculate the time to ninety-five percent pathogen reduction, we simulate the model forward in time deterministically, starting at the pathogen endemic steady state (see Supplementary Information) with the following parameter values:  $d = 0.00274 \text{ day}^{-1}$ ,  $b = 1.37 \text{ day}^{-1}$ . We chose the value of  $d$  to reflect the typical lifespan of individuals in the *Mus* genus [68] and chose  $b$  to reflect a constant population size of 500 individuals. Each simulation was initialized with a number of exposed individuals equal to ten percent of the susceptible population. Model simulations are carried out until the number of pathogen infected individuals is equal to five percent of the original starting value.

### 2.5.5 ESTIMATING EPIDEMIOLOGICAL PARAMETERS FOR LASV AND LCMV

We estimated epidemiological parameters for Lassa virus and Lymphocytic Choriomeningitis virus using published serological data and duration of infection estimates from previous studies [50, 51]. Similar to section 2.5.3, we find the the steady state solutions to our general pathogen model, and identify the solution where the pathogen is endemic. We then solve this quantity for the fraction of individuals that are susceptible, and input our LASV and LCMV seroprevalence data to get estimates for the transmission

rate of each. The solution is

$$\beta_w = \frac{(d + \gamma)}{(1 - p)}, \quad (2.12)$$

where  $p$  is the seroprevalence for the given pathogen,  $d = 0.00274 \text{ day}^{-1}$ , and  $\gamma$  is drawn from LASV and LCMV literature (LASV:  $1/\gamma=22$  days [50], LCMV:  $1/\gamma=365$  days [51]).

## 2.6 SUPPLEMENTAL INFORMATION

This section provides further details on the methods used to evaluate the effectiveness of an MCMV-vectored transmissible vaccine. To this end, we detail model modifications that were used for the ABC process, we provide further details regarding the ABC algorithm itself, and we detail the steady state solutions to our model that give rise to the vaccine and pathogen basic reproductive numbers.

### 2.6.1 PARTIAL VACCINE EFFICACY

To account for partial vaccine efficacy, we develop an extended model that allows for co-infection between the transmissible vaccine and the pathogen, where the vaccine has the capacity to only partially block pathogen transmission. In this model, individuals that have been exposed ( $E$ ), as well as those that are actively infectious with the vaccine ( $V$ ), can be infected by the target pathogen. In these cases, individuals transition into the vaccine-exposed pathogen-infected class ( $E_w$ ), and the vaccine-infectious pathogen-infected class ( $V_w$ ). From these co-infected classes, pathogen transmission is reduced by a factor of  $(1 - \rho)$ . When  $\rho = 1$ , the vaccine perfectly blocks pathogen transmission and the co-infection model reduces to the original pathogen and vaccine model described in the main text. Further, individuals in the  $E_w$  and  $V_w$  classes can recover from pathogen infection and transition into the  $E_r$  and  $V_r$  classes, respectively. Moreover, all individuals that have been exposed to the vaccine ( $E$ ,  $E_w$ , and  $E_r$ ), transition into their corresponding vaccine infectious class at rate  $\alpha_1$ . All model parameters are described in the main text

(i.e.,  $\beta_v$ ,  $\alpha_1$ ,  $\beta_w$ ,  $\gamma$ ,  $b$ ,  $d$ ). These assumptions lead to the following extended model of co-infection:

$$\frac{dS}{dt} = b - \frac{\beta_w SW}{N} - \frac{(1-\rho)\beta_w SE_w}{N} - \frac{\beta_v SV_w}{N} - \frac{(1-\rho)\beta_w SV_w}{N} - \frac{\beta_v SV_r}{N} - \frac{\beta_v SV}{N} - dS \quad (2.13)$$

$$\frac{dE}{dt} = \frac{\beta_v SV}{N} + \frac{\beta_v SV_w}{N} + \frac{\beta_v SV_r}{N} - \frac{\beta_w EW}{N} - \frac{(1-\rho)\beta_w EV_w}{N} - \frac{(1-\rho)\beta_w EE_w}{N} - \alpha_1 E - dE \quad (2.14)$$

$$\frac{dE_w}{dt} = \frac{\beta_w EW}{N} + \frac{(1-\rho)\beta_w EV_w}{N} + \frac{(1-\rho)\beta_w EE_w}{N} - \alpha_1 E_w - \gamma E_w - dE_w \quad (2.15)$$

$$\frac{dE_r}{dt} = \gamma E_w - \alpha_1 E_r - dE_r \quad (2.16)$$

$$\frac{dV}{dt} = \alpha_1 E - \frac{\beta_w VW}{N} - \frac{(1-\rho)\beta_w VV_w}{N} - \frac{(1-\rho)\beta_w VE_w}{N} - dV \quad (2.17)$$

$$\frac{dV_w}{dt} = \frac{\beta_w VW}{N} + \frac{(1-\rho)\beta_w VV_w}{N} + \frac{(1-\rho)\beta_w VE_w}{N} + \alpha_1 E_w - \gamma V_w - dV_w \quad (2.18)$$

$$\frac{dV_r}{dt} = \gamma V_w + \alpha_1 E_r - dV_r \quad (2.19)$$

$$\frac{dW}{dt} = \frac{\beta_w SW}{N} + \frac{(1-\rho)\beta_w SE_w}{N} + \frac{(1-\rho)\beta_w SV_w}{N} - \gamma W - dW \quad (2.20)$$

$$\frac{dR}{dt} = \gamma W - dR. \quad (2.21)$$

To solve for the critical vaccine efficacy that must be achieved for a transmissible vaccine to protect a reservoir population from pathogen invasion, we linearized the pathogen-infected subsystem ( $E_w$ ,  $V_w$ ,  $W$ ) about the pathogen-free steady state. We then solved for the vaccine efficacy ( $\rho$ ) that leads to a positive eigenvalue of the Jacobian matrix of this linearized subsystem.

## 2.6.2 MODEL MODIFICATIONS FOR ABC

To estimate the epidemiological parameters of MCMV from the time series data set, we implement a continuous time Markov chain (CTMC) version of the model described in the main text, with some small modifications to the base model. Briefly, the CTMC

version of our model is a stochastic process where the state variables are discrete random variables and the time scale is continuous [69]. We simulate the model using the Gillespie algorithm, where time increases incrementally by some small random value  $\Delta t$ . At each time interval there is a probability of transitioning from any given state, dependent on the various parameters found in the model (Table 2.2). For this implementation of the model, we remove the birth and death rates due to the relatively constant population size of the founder population observed by Farroway et al. (2002). Further, we include an additional exposed class ( $E_2$ ) to account for the initial fraction of the population that was exposed to MCMV via IP injection. We include the additional exposed class because exposure via transmission and IP injection are biologically different. With the addition of the IP injected class ( $E_2$ ), we introduce another parameter,  $\alpha_2$ , which defines that rate at which IP injected individuals become infectious.

<b>Event</b>	<b>Transition</b>	<b>Transition Rate</b>
Susceptible infected with MCMV	$S \rightarrow S - 1, E_1 \rightarrow E_1 + 1$	$\frac{\beta_v V}{N}$
Exposed via transmission becomes infectious	$E_1 \rightarrow E_1 - 1, V \rightarrow V + 1$	$\alpha_1$
Exposed via IP injection becomes infectious	$E_2 \rightarrow E_2 - 1, V \rightarrow V + 1$	$\alpha_2$

Table 2.2: The possible events, transitions, and transition rates found in the CTMC model.

### 2.6.3 APPROXIMATE BAYESIAN COMPUTATION

As stated in the main text, we use Approximate Bayesian Computation in combination with the time series data set described by Farroway et al. (2002) to produce baseline parameter estimates for MCMV. We begin the ABC process by taking a random sample of the parameter values found in the prior distributions (described in Table 2.3). These

priors were determined based on plausible values found in MCMV literature. These parameter samples are then fed into the CTMC model, and the model is simulated forward in time. Model simulations were initiated according to the initial conditions described in Farroway et al. (2002) ( $S = 16$ ,  $E_1 = 0$ ,  $E_2 = 6$ ,  $V = 0$ ). We stop the simulations once the time in the model has reached 84 days (the last time step described in Farroway et al. (2002)), and we take a binomial sample of the number of infectious individuals at each time point detailed in the data set, according to the sampling effort for a given rodent enclosure. We take a binomial sample at each time point in an attempt to recreate the possibility for sampling error in the MCMV transmission experiments. The binomial distribution is chosen for our sampling, as an individual is either MCMV positive (1) or negative (0) at each time point. We then calculate the total sum of squares (TSS) for our simulated sample across all enclosures at a given time point, and then averaged the TSS across all time points. The resulting quantity is a measure of how well the parameter samples and simulated model perform against the actual transmission experiments. If this value was less than or equal to our acceptance criteria (0.1), then the parameters for that simulated run were added to the multivariate posterior distribution. The ABC process was carried out until the multivariate posterior distribution accumulated twenty five thousand samples.



Parameter	Prior	Justification
$\beta_v$	Uniform on [0.0005, 0.009]	The range was determined based on values that could plausibly lead to the observed seroprevalence.
$\alpha_1$	Gamma with mean 0.099 and shape 3	The mode was selected based on known MCMV seroconversion [70].
$\alpha_2$	Gamma with mean .099 and shape parameter 100	The mode was selected based on the seroconversion of MCMV injected via IP injection [70].

Table 2.3: Prior distributions for each parameter in the MCMV model.

#### 2.6.4 STEADY STATE MODEL SOLUTIONS

Many of the results in this manuscript are reliant on the steady state solutions to our model of MCMV and pathogen spread. Steady state solutions, also known as equilibria, are solutions of the differential equations that are constant with respect to time. To find these steady states, we set the left hand side of the equations in the main text to zero, and solved the resulting algebraic equations for each of the state variables. These analyses identify three steady state solutions. The first,

$$S = \frac{b(d + \alpha_1)}{\alpha_1\beta_v} \quad (2.22)$$

$$E = \frac{-bd^2 - bd\alpha_1 + b\alpha_1\beta_v}{\alpha_1(d + \alpha_1)\beta_v} \quad (2.23)$$

$$V = \frac{-bd^2 - bd\alpha_1 + b\alpha_1\beta_v}{d(d + \alpha_1)\beta_v} \quad (2.24)$$

$$W = 0 \quad (2.25)$$

$$R = 0, \quad (2.26)$$

the second,

$$S = \frac{b(d + \gamma)}{d\beta_w} \quad (2.27)$$

$$E = 0 \quad (2.28)$$

$$V = 0 \quad (2.29)$$

$$W = \frac{-bd - b\gamma + b\beta_w}{(d + \gamma)\beta_w} \quad (2.30)$$

$$R = -\frac{b\gamma(d + \gamma - \beta_w)}{d(d + \gamma)\beta_w}, \quad (2.31)$$

and the third,

$$S = \frac{b}{d} \quad (2.32)$$

$$E = 0 \quad (2.33)$$

$$V = 0 \quad (2.34)$$

$$W = 0 \quad (2.35)$$

$$R = 0. \quad (2.36)$$

From these solutions, we see that there are three possible scenarios, 1.) the vaccine is endemic and the pathogen is absent, 2.) the pathogen is present and the vaccine is absent, and 3.) both the pathogen and vaccine are absent from the population.

### 2.6.5 CALCULATING BASIC REPRODUCTIVE NUMBERS

The basic reproductive number for a transmissible agent, also known as  $R_0$ , is classically defined as the number of secondary infections produced by a single infectious individual in a completely susceptible population [71]. This quantity is important, as it provides insight into whether or not a transmission capable virus will successfully spread in a population. For example, we know that when  $R_0 > 1$ , a virus has the ability to

successfully invade a population, and when  $R_0 < 1$  a virus will fail to undergo sustained transmission in the population.

To find the analytical solution for the basic reproductive number of MCMV and the pathogen, we performed a standard stability analysis on the infection free steady state. To perform this analysis, we linearized the system of differential equations found in the main text, and evaluated the resulting Jacobian matrix at the equilibrium solution (equations (2.32-2.36)). We then found the set of eigenvalues for the resulting matrix, and determined the leading eigenvalue from the set. From this quantity, we were able to find the threshold transmission conditions that lead to the instability of the infection free steady state:

$$\frac{\beta_v \alpha_1}{d(d + \alpha_1)} > 1, \quad (2.37)$$

or

$$\frac{\beta_w}{d + \gamma} > 1. \quad (2.38)$$

According to the classic definition of  $R_0$ , the quantity defined by equation (2.37) is MCMV's reproductive number ( $R_{0,v}$ ). Similarly, equation (2.38) represents the reproductive number of the pathogen ( $R_{0,w}$ ).

For completeness, we performed a stability analysis on the MCMV endemic steady state (equations (2.22-2.26)) and the pathogen endemic steady state (equations (2.27-2.31)). We found that the vaccine endemic steady state is stable if

$$R_{0,v} > 1, \quad (2.39)$$

and

$$R_{0,v} > R_{0,w}. \quad (2.40)$$

Further, we find that the pathogen endemic steady state is stable if

$$R_{0,w} > 1, \tag{2.41}$$

and

$$R_{0,w} > R_{0,v}. \tag{2.42}$$

## CHAPTER 3: FACILITATING OPEN SCIENCE IN LASSA VIRUS RESEARCH

### 3.1 ABSTRACT

Lassa virus spillover into human populations is a significant burden on human health across West Africa, with thousands of deaths occurring each year. Implementing effective virus control measures relies on comprehensive data sets that detail viral sampling across space and time, something that is currently lacking in Lassa virus research. To address the gap in open-source Lassa data sets, we have compiled publicly available data on the distribution of Lassa virus across West Africa. We integrate these data into a database with an accompanying dashboard that facilitates interactive data visualizations, and contains tools that allow for easy data management (i.e, download and upload). Along with promoting scientific collaboration within Lassa virus research, our database and data visualizations identify key gaps in the sampling effort of Lassa virus across space and time.

### 3.2 INTRODUCTION

Lassa virus is a zoonotic pathogen that infects hundreds of thousands of humans across West Africa each year resulting in thousands of deaths [35, 72]. The virus is maintained by the reservoir species *Mastomys natalensis*, where transmission to humans is facilitated by exposure to rodent feces and urine, often occurring in human habitation [47, 73]. Although *Mastomys natalensis* are the primary reservoir for Lassa virus, the pathogen has been shown to persist in other rodent species as well [74, 75]. Given the widespread impact that Lassa virus has on West Africa, it is critical that forecasting tools are developed to help evaluate the risk of the virus across space and time, as well as to help guide the implementation of virus control measures [76, 77].

The development of spatio-temporal forecasting tools are reliant on detailed data sets that describe viral sampling at both a temporal and geographic scale. To date, the number

of high resolution Lassa virus data sets is limited [76,78]. Although these studies are of considerable importance, they exist in a static form such that once published, they are no longer updated and are not easily accessed by the community of Lassa researchers. This is problematic, as Lassa virus infection in both humans and rodents continues to vary across space and time [79], meaning that Lassa data collections need to be updated regularly. Further, given the significant role that dynamic data sets play in the modeling of infectious disease, it is important that such data sets can be accessed by a community of researchers. Developing tools that facilitate easy data access promotes scientific collaboration, and rapidly advances contributions to public health [80].

To address the lack of regularly updated, open-source Lassa data sets, we have compiled publicly available data on the distribution of Lassa virus across West Africa. Our data set includes viral prevalence data compiled from peer-reviewed publications, and viral sequence data retrieved from GenBank. These data have been collected and curated with modeling in mind, resulting in a highly processed, high quality data product. To promote the use of our data set, we have developed software that allows the Lassa virus database to be easily updated, and a web interface that provides tools to visualize and download the entirety of the database. In this study, we will highlight the data collection and storage processes, provide metrics on the spatial and temporal distribution of our data set, and further highlight the tools that we have developed to promote user interaction with the Lassa virus database.

## 3.3 METHODS

### 3.3.1 LASSA VIRUS DATA COLLECTION AND STORAGE

Described in a recent article [77], our data set is comprised of Lassa virus prevalence data found in peer-reviewed publications and sequence data described in GenBank [81]. Throughout this study, we refer to the Lassa virus prevalence data as “viral infection data”. We describe viral infection data as Lassa virus prevalence that was determined

via serology (previous infection according to arenavirus antibodies) and/or PCR (current infection with Lassa virus). Further, we refer to the distinct subset of GenBank Lassa virus sequence data as “viral sequence data”.

To draw viral infection data from literature and viral sequence data from GenBank, we developed Excel templates that describe the key data fields that are to be extracted from each data source. Some of the important fields that were incorporated into the viral infection template include the latitude and longitude of the sample, the year, month, and day that the sample was taken, the antibody target, the diagnostic method that was utilized (i.e., ELISA, IFA, PCR), the prevalence of Lassa virus, a citation to the source study, and the host species that was sampled. Similarly, important information in the Lassa sequence template includes the sequence itself, the latitude and longitude of where the virus came from, the country where the sequence was taken, information about the GenBank identification, the host species that the virus was extracted from, and the year that the sequence was collected. The full extent of the data templates can be found at <https://github.com/tvarrelman/LassaMapping/tree/master/LassaMappingApp/static>.

Next, to compile our data templates into a single source location, we developed a pipeline to feed the Lassa virus data into a MySQL database [82]. Within the database, we chose to adopt a relational data model, which allows static fields such as country names and references to exist in their own table with a unique id that ties values to the Lassa infection and sequence tables (Figure 3.1). This process reduces the possibility of including inaccuracies in key data fields. Further, we have developed a straightforward user interface that allows Lassa data to be uploaded into the database using CSV files that follow the same structure as the data templates described above. However, if the data fields in the CSV file do not match those described in our templates, the file will not be uploaded to the database. As a final quality check we require that each data field in the prospective template be of a specific data type, otherwise the data upload will be rejected.

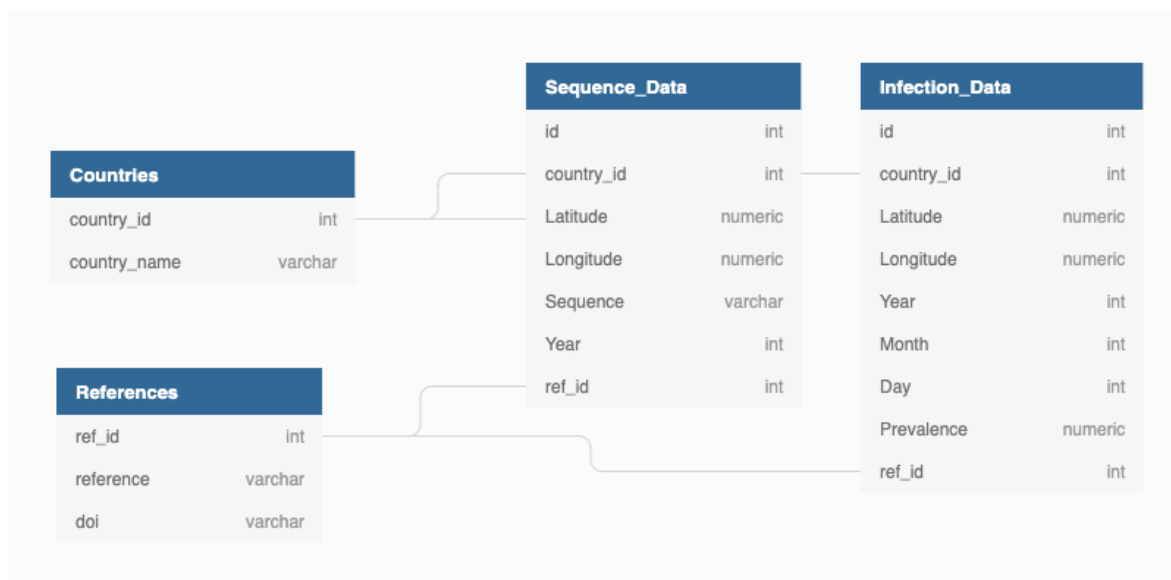


Figure 3.1: Structure of the Lassa data in the MySQL database. We create separate tables for the country names, the reference studies, the sequence data, and the infection data. Within the sequence and infection tables, there is a `country_id` and `reference_id` that point to the values found in the country and reference tables, respectively. Note, data fields within the sequence and infection table are omitted from this visualization.

### 3.3.2 LASSA VIRUS INTERACTIVE DASHBOARD

To develop the web-interface that is paired with the Lassa virus database, we relied on several programming languages and web development tools. Specifically, we utilized the Flask web framework to develop the application itself [83, 84], and leveraged HTML markup language for designing the layout of our web-page. We harnessed the power of the JavaScript programming language to develop the dynamic features on our dashboard [85, 86]. Data visualizations include interactive Leaflet maps and summary statistics displayed in Plotly charts [87, 88]. Source code for the project can be found at <https://github.com/tvarrelman/LassaMapping>.



## 3.4 RESULTS

### 3.4.1 SPATIAL AND TEMPORAL DISTRIBUTION OF LASSA VIRUS

Currently, publicly available viral infection data spans eight countries across West Africa, with sample years ranging from 1970-2016. These countries include Benin, Côte d'Ivoire, Ghana, Guinea, Liberia, Mali, Nigeria, and Sierra Leone. The viral infection data consists of serosurveys from 94 human sampled locations and features serology and Lassa virus detection from 80 rodent sampled locations (Figure 3.2). We chose to limit the viral infection data in humans to only include data points that were studied in serosurveys, as they provide the optimal type of data that can be integrated into mechanistic models. For example, the human serosurveys that we include detail locations where humans were randomly sampled for arenavirus antibodies. This data therefore accounts for potential sampling biases, includes a latitude and longitude of the sampling location, and includes accurate sampling dates. In the data collection process, we ensured that the viral infection data from rodents is of similar quality to the human data. In total, our data set consists of Lassa virus prevalence data from 12,711 humans and 4,546 rodents, stemming from 7 human studies [47, 89–94], and 11 rodent studies [47, 75, 95–103].

Country	# Rodent Sample Locations	# Human Sample Locations
Benin	2	0
Côte d'Ivoire	7	0
Ghana	9	10
Guinea	20	58
Liberia	0	7
Mali	17	3
Nigeria	9	0
Sierra Leone	16	16

Table 3.1: Sample locations of Lassa virus prevalence data. Currently, the viral infection data set consists of human serosurveys from 94 locations, and rodent serology and virus extraction from 80 locations.

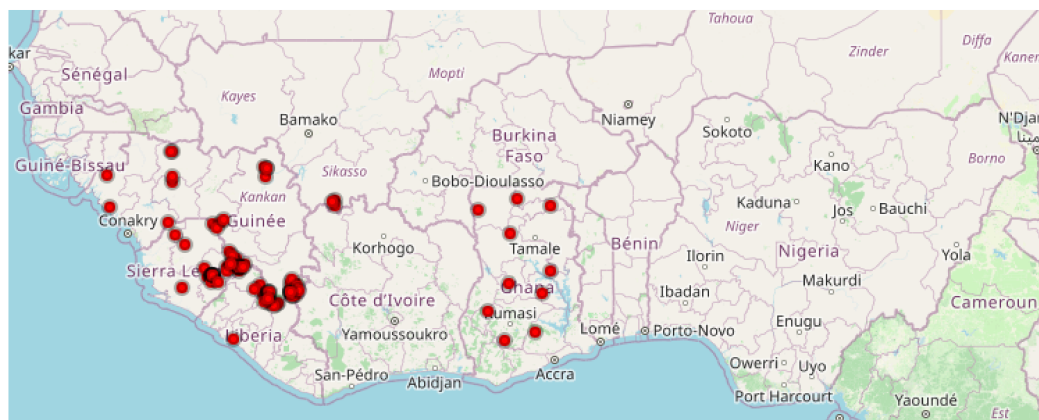
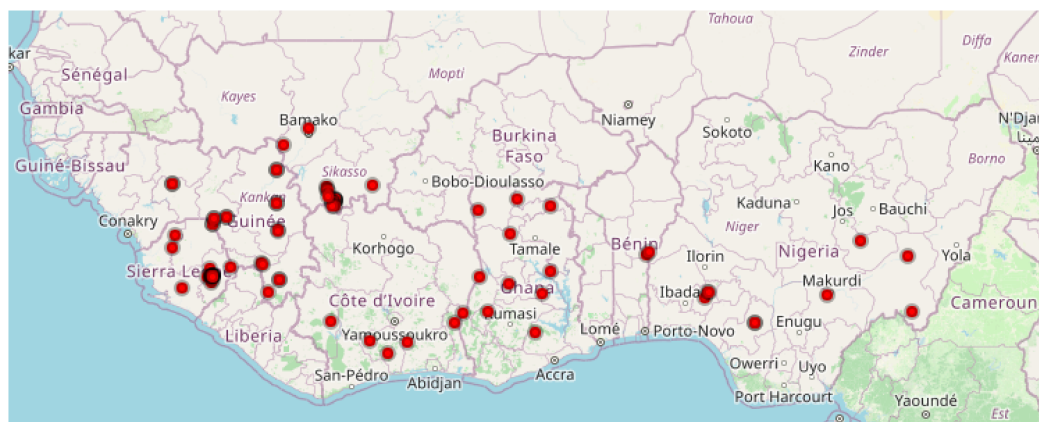
**a****Viral Infection: Humans****b****Viral Infection: Rodents**

Figure 3.2: a.) 94 sample locations from seven human serosurveys. b.) 80 sample locations for rodent serology and virus detection. Note that overlapping sample locations results in a darker band around the red data points.

Similar to the viral infection subset of our data, the viral sequence data also spans eight countries across West Africa. These eight countries include Benin, Ghana, Guinea, Liberia, Mali, Nigeria, Sierra Leone, and Togo. Sequences available in GenBank were sampled over a span of 44 years (1975-2019), and include 85 Lassa sequences taken from human hosts and 494 sequences from rodent hosts (Figure 3.3). We include an additional 956 sequences in the database that do not have an associated latitude and longitude. These sequences are still included, as they have an associated country name and may be useful for modeling sequence diversity across broad spatial units. Although not all

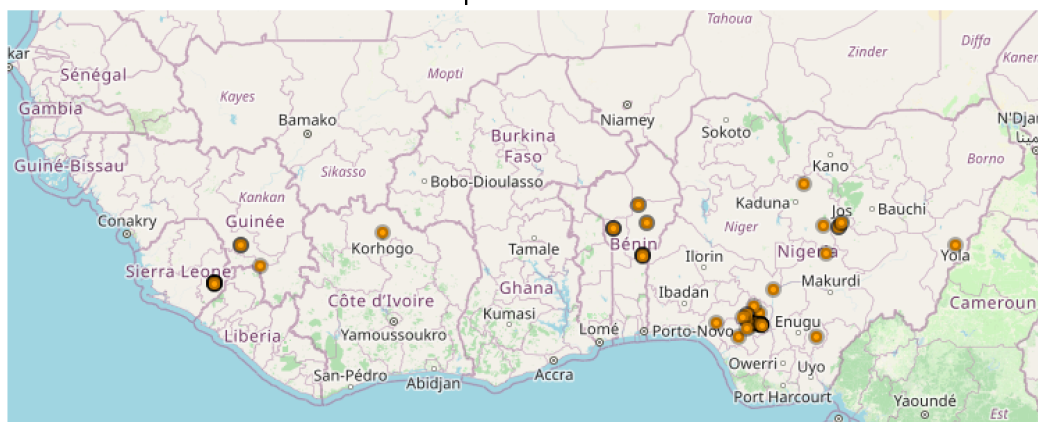
GenBank entries come from published studies, our data set includes information from 17 publications [74, 98, 100, 101, 104–116].

<b>Country</b>	<b># Sequences From Humans</b>	<b># Sequences From Rodents</b>
Benin	18	6
Ghana	0	4
Guinea	12	250
Liberia	81	0
Mali	3	22
Nigeria	872	85
Sierra Leone	38	138
Togo	6	0

Table 3.2: Number of Lassa virus sequences sampled from each of the eight countries represented in the data set. Not all samples represented in this table are present in our mapping, as a large majority of sequences lack an associated latitude and longitude.

**a**

## Viral Sequences: Humans

**b**

## Viral Sequences: Rodents

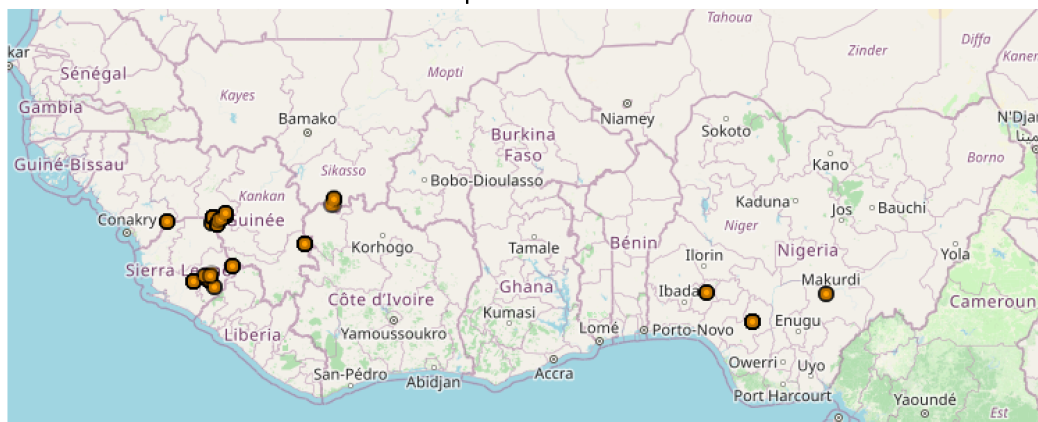


Figure 3.3: Sample locations of viral sequences across West Africa. Our data set currently consists of 579 Lassa sequences that have spatially explicit meta data (85 from human hosts and 494 from rodent hosts). Note that overlapping sample locations results in a darker band around the orange data points.

### 3.4.2 INTERACTIVE LASSA VIRUS DASHBOARD

To visualize our dynamic Lassa data set, we provide interactive maps that allow users to select data points and view the associated meta data. Such meta data varies according to the type of data (viral infection vs. viral sequence), and includes information regarding the source of the data point, and either the prevalence of Lassa virus or the GenBank information required to look up the sequence. Further, our interactive maps can be filtered by the collection year, allowing users to understand the temporal distribution of

the data. Accompanying the interactive maps, we provide time-series plots that describe the prevalence of Lassa virus and the diagnostic methods that were used to determine that prevalence. We also provide time-series plots describing the number of Lassa sequences that exist in our database. Figure 3.4 depicts data visualizations that can be found on the Lassa virus dashboard (<https://lassa.nkn.uidaho.edu>).

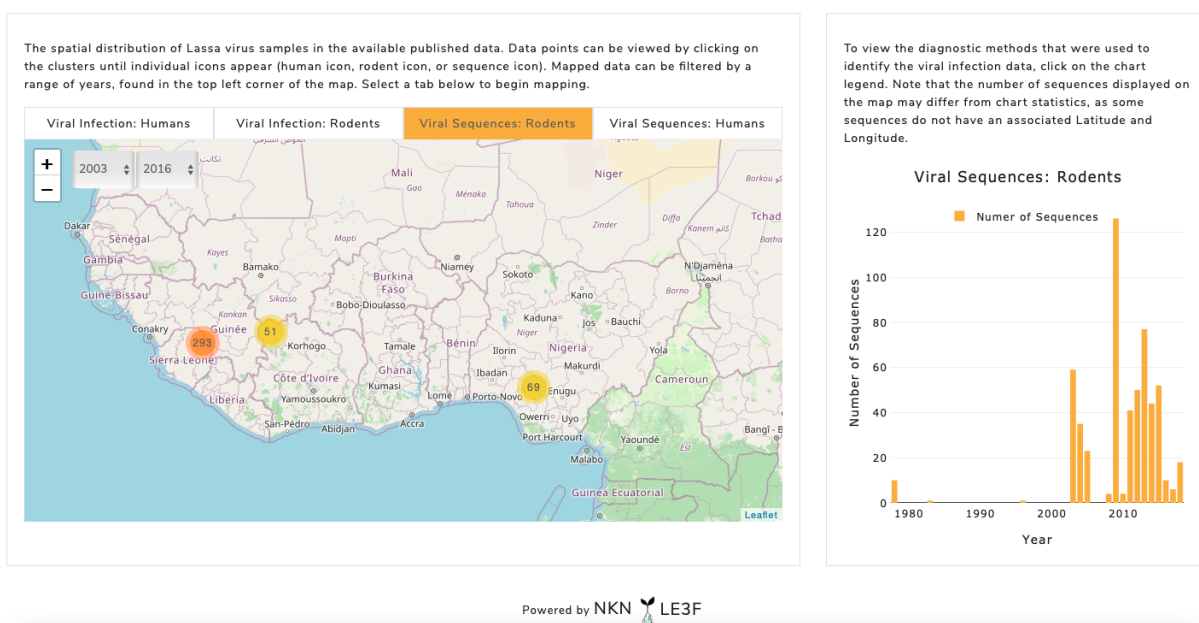


Figure 3.4: Visualization of the Lassa virus dashboard.

In addition to data visualization, our dashboard provides an intuitive user interface for filtered data download. Filter options include the type of data (viral infection vs. viral sequence), the countries that should be included in the download, and also a range of collection years. Selecting all filter options will download the entirety of the database.

### 3.5 DISCUSSION

We have developed an extensive Lassa virus database that describes the distribution of Lassa virus across space and time. Our product includes a web-interface that allows users to visualize the extent of the data, and we provide tools that allow for easy data management (i.e. download and upload). While developing these tools, we included the

necessary checks to ensure that only quality data can be loaded into the Lassa database. Users can request to upload their own Lassa virus data set by sending an email to the Nuismer lab with an attached CVS template. The requested upload must meet our template format and pass a screening by one of the product administrators. Database maintenance will be performed by the Nuismer lab at the University of Idaho with the support of the Northwest Knowledge Network.

Although our database represents the first open source Lassa virus data product of its kind, there are still critical gaps in the spatial extent of our data collection. For example, it is well known that Nigeria is a country that is heavily impacted by Lassa virus each year [35,117]; however it is a region that is largely underrepresented in our viral infection data set. The lack of representation stems from the complete absence of high quality human serosurveys from Nigerian communities. Gaps in the spatial extent of our database are further highlighted by the distribution of Lassa virus sequences. Specifically, sequences are primarily found in three countries (Sierra Leone, Guinea, and Nigeria). It is unclear if this spatial bias results from the true distribution of Lassa virus across West Africa or from sampling bias. Further, we find that the number of sequences sampled across different countries varies wildly between human and rodent hosts. For example, the majority of rodent sequences stem from Guinea, whereas most sequences extracted from humans come from Nigeria. This is problematic, as modeling something such as viral spillover will likely require a large number of Lassa sequences from rodents and humans in the same locations.

While our database does contain data points that detail the prevalence of specifically Lassa virus, our product also contains a large number of data points that were derived using serology. Serology is a process where a serum sample is tested for antibodies to particular family of viruses. In our case, these data points were tested for general arenavirus infection, and not specifically Lassa virus. Therefore, there is ambiguity in the true identity of the infection that led to these data points. However, given the context of

the source studies, we believe that Lassa infection was likely.

Open source disease data sets and visualization are crucial for driving the advancement of disease modeling and public health decision making. Constructing comprehensive data sets requires researchers to painstakingly comb through literature and curate common data files, a process that can take hundreds of hours. Saving researchers this time, allows the focus to be on developing novel tools for forecasting and data analysis.



## REFERENCES

- [1] Kate E Jones, Nikkita G Patel, Marc A Levy, Adam Storeygard, Deborah Balk, John L Gittleman, and Peter Daszak. Global trends in emerging infectious diseases. *Nature*, 451:990–993, 2008.
- [2] Yoshimi Tsuda, Christopher J Parkins, Patrizia Caposio, Friederike Feldmann, Sara Botto, Susan Ball, Ilhem Messaoudi, Luka Cicin-Sain, Heinz Feldmann, and Michael A Jarvis. A cytomegalovirus-based vaccine provides long-lasting protection against lethal Ebola virus challenge after a single dose. *Vaccine*, 33(19):2261–2266, 2015.
- [3] CDC. Ebola (Ebola virus disease). <https://www.cdc.gov/vhf/ebola/outbreaks/2014-west-africa/cost-of-ebola.html>, 2016.
- [4] Christian Gortazar, Iratxe Diez-Delgado, Jose Angel Barasona, Joaquin Vicente, Jose De La Fuente, and Mariana Boadella. The wild side of disease control at the wildlife-livestock-human interface: A review. *Frontiers in Veterinary Science*, 1:27, 2015.
- [5] Joanne Maki, Anne-Laure Guiot, Michel Aubert, Bernard Brochier, Florence Cliquet, Cathleen A Hanlon, Roni King, Ernest H Oertli, Charles E Rupprecht, Caroline Schumacher, Dennis Slate, Boris Yakobson, Anne Wohlers, and Emily W Lankau. Oral vaccination of wildlife using a vaccinia–rabies-glycoprotein recombinant virus vaccine (RABORAL V-RG®): a global review. *Veterinary Research*, 48(1):57, 2017.
- [6] Petra Oyston and Karen Robinson. The current challenges for vaccine development. *Journal of Medical Microbiology*, 61(7):889–894, 2012.

- [7] Aisling A Murphy, Alec J Redwood, and Michael A Jarvis. Self-disseminating vaccines for emerging infectious diseases. *Expert Review of Vaccines*, 15(1):31–39, 2015.
- [8] Scott L Nuismer, Benjamin M Althouse, Ryan May, James J Bull, Sean P Stromberg, and Rustom Antia. Eradicating infectious disease using weakly transmissible vaccines. *Proceedings of the Royal Society of London B: Biological Sciences*, 283(1841), 2016.
- [9] Andrew J Basinski, Tanner J Varrelman, Mark W Smithson, Ryan H May, Christopher H Remien, and Scott L Nuismer. Evaluating the promise of recombinant transmissible vaccines. *Vaccine*, 36(5):675–682, 2018.
- [10] Scott L. Nuismer, Ryan May, Andrew Basinski, and Christopher H. Remien. Controlling epidemics with transmissible vaccines. *PLOS ONE*, 13(5):1–13, 05 2018.
- [11] Sara H Paull, Sejin Song, Katherine M McClure, Loren C Sackett, A Marm Kilpatrick, and Pieter TJ Johnson. From superspreaders to disease hotspots: linking transmission across hosts and space. *Frontiers in Ecology and the Environment*, 10(2):75–82, 2012.
- [12] Roy M Anderson and Robert M May. Spatial, temporal, and genetic heterogeneity in host populations and the design of immunization programmes. *Mathematical Medicine and Biology: A Journal of the IMA*, 1(3):233–266, 1984.
- [13] Vincent T Metzger, James O Lloyd-Smith, and Leor S Weinberger. Autonomous targeting of infectious superspreaders using engineered transmissible therapies. *PLOS Computational Biology*, 7(3):1–12, 2011.
- [14] Roy M Anderson and Robert M May. *Infectious Diseases of Humans: Dynamics and Control*. Oxford University Press, 1991.

- [15] Matt J Keeling and Pejman Rohani. *Modeling Infectious Diseases in Humans and Animals*. Princeton University Press, 2007.
- [16] Jong-Hoon Kim and Seong-Hwan Rho. Transmission dynamics of oral polio vaccine viruses and vaccine-derived polioviruses on networks. *Journal of Theoretical Biology*, 364(7):266–274, 2015.
- [17] James J Bull, Mark W Smithson, and Scott L Nuismer. Transmissible viral vaccines. *Trends in Microbiology*, 26(1):6–15, 2018.
- [18] Peter Caley and Jim Hone. Assessing the host disease status of wildlife and the implications for disease control: Mycobacterium bovis infection in feral ferrets. *Journal of Applied Ecology*, 42(4):708–719, 2005.
- [19] Nancy E McIntyre, Yong-Kyu Chu, Owenm Robert D, Alisa Abuzeineh, Noe De La Sancha, Carl W Dick, Tyla Holsomback, Richard A Nisbett, and Colleen Jonsson. A longitudinal study of Bayou virus, hosts, and habitat. *The American Journal of Tropical Medicine and Hygiene*, 73(6):1043–1049, 2005.
- [20] FR Adler, CA Clay, and EM Lehmer. The role of heterogeneity in the persistence and prevalence of Sin Nombre virus in deer mice. *The American Naturalist*, 172(6):855–867, 2008.
- [21] The Jarvis Lab. Our research: Disseminating zbvs. <http://www.thejarvislab.com/research/>, 2018.
- [22] O Diekmann, JAP Heesterbeek, and MG Roberts. The construction of next-generation matrices for compartmental epidemic models. *Journal of the Royal Society Interface*, 47(7):873–885, 2010.
- [23] Adam MacNeil, Stuart T Nichol, and Christina F Spiropoulou. Hantavirus pulmonary syndrome. *Virus Research*, 162(1-2):138–147, 2011.

- [24] CDC. Hantavirus. <https://www.cdc.gov/hantavirus/>, 2018.
- [25] Mausumi Bharadwaj, Katy Mirowsky, Chunyan Ye, Jason Botten, Barbara Masten, Joyce Yee, C. Richard Lyons, and Brian Hjelle. Genetic vaccines protect against Sin Nombre hantavirus challenge in the deer mouse (*Peromyscus maniculatus*). *Journal of General Virology*, 83(7):1745–1751, 2002.
- [26] Albert A Rizvanov, Svetlana F Khaiboullina, Albert GM van Geelen, and Stephen C St. Jeor. Replication and immunoactivity of the recombinant *Peromyscus maniculatus* cytomegalovirus expressing hantavirus G1 glycoprotein in vivo and in vitro. *Vaccine*, 24(3):327–334, 2006.
- [27] JN Mills, TG Ksiazek, CJ Peters, and JE Childs. Long-term studies of hantavirus reservoir populations in the southwestern United States: A synthesis. *Emerging Infectious Diseases*, 5(1):135–142, 1999.
- [28] USDA. United States Department of Agriculture (USDA) national rabies management program summary. [https://www.aphis.usda.gov/wildlife\\_damage/oral\\_rabies/downloads/NationalReport\\_2006.pdf](https://www.aphis.usda.gov/wildlife_damage/oral_rabies/downloads/NationalReport_2006.pdf), 2006.
- [29] USDA. United States Department of Agriculture (USDA) national rabies management program summary. [https://www.aphis.usda.gov/wildlife\\_damage/oral\\_rabies/downloads/NationalReport\\_2007.pdf](https://www.aphis.usda.gov/wildlife_damage/oral_rabies/downloads/NationalReport_2007.pdf), 2007.
- [30] USDA. United States Department of Agriculture (USDA) national rabies management program summary. [https://www.aphis.usda.gov/wildlife\\_damage/oral\\_rabies/downloads/NationalReport\\_2008.pdf](https://www.aphis.usda.gov/wildlife_damage/oral_rabies/downloads/NationalReport_2008.pdf), 2008.
- [31] USDA. United States Department of Agriculture (USDA) national rabies management program summary. [https://www.aphis.usda.gov/wildlife\\_damage/oral\\_rabies/downloads/NationalReport\\_2009.pdf](https://www.aphis.usda.gov/wildlife_damage/oral_rabies/downloads/NationalReport_2009.pdf), 2009.

- [32] USDA. United States Department of Agriculture (USDA) national rabies management program summary. [https://www.aphis.usda.gov/wildlife\\_damage/oral\\_rabies/downloads/NationalReport\\_2010.pdf](https://www.aphis.usda.gov/wildlife_damage/oral_rabies/downloads/NationalReport_2010.pdf), 2010.
- [33] Yan-Rong Guo, Qing-Dong Cao, Zhong-Si Hong, Yuan-Yang Tan, Shou-Deng Chen, Hong-Jun Jin, Kai Sen Tan, De-Yun Wang, and Yan Yan. The origin, transmission and clinical therapies on coronavirus disease 2019 (COVID-19) outbreak - an update on the status. *Military Medical Research*, 7, 12 2020.
- [34] Centers for Disease Control and Prevention. Lassa fever. <https://www.cdc.gov/vhf/lassa/index.html>, 2019.
- [35] Sanjeet Bagcchi. Lassa fever outbreak continues across Nigeria. *The Lancet Infectious Diseases*, 20(5):543, 2020.
- [36] Joachim Mariën, Benny Borremans, Fodé Kourouma, Jatta Baforday, Toni Rieger, Stephan Günther, N’Faly Magassouba, Herwig Leirs, and Elisabeth Fichet-Calvet. Evaluation of rodent control to fight Lassa fever based on field data and mathematical modelling. *Emerging Microbes & Infections*, 8(1):640–649, 2019.
- [37] Conrad M. Freuling, Katie Hampson, Thomas Selhorst, Ronald Schröder, Francois X. Meslin, Thomas C. Mettenleiter, and Thomas Müller. The elimination of fox rabies from Europe: determinants of success and lessons for the future. *Philosophical Transactions of the Royal Society B: Biological Sciences*, 368(1623):20120142, 2013.
- [38] Scott Nuismer and James Bull. Self-disseminating vaccines to suppress zoonoses. *Nature Ecology & Evolution*, 4:1–6, 07 2020.
- [39] Geoffrey R. Shellam. The potential of murine cytomegalovirus as a viral vector for immunocontraception. *Reproduction, Fertility and Development*, 6(3):401–419, 1994.

- [40] Michael A. Jarvis, Scott G. Hansen, Jay A. Nelson, Louis J. Picker, and Klaus Früh. Vaccine vectors using the unique biology and immunology of cytomegalovirus. In Matthias J. Reddehase and Niels A.W. Lemmermann, editors, *Cytomegaloviruses From Molecular Pathogenesis to Intervention*, volume 2, chapter 21, pages 450–461. Caister Academic Press, Norfolk, UK, 2013.
- [41] Tanner J. Varrelman, Andrew J. Basinski, Christopher H. Remien, and Scott L. Nuismer. Transmissible vaccines in heterogeneous populations: Implications for vaccine design. *One Health*, 7:100084, 2019.
- [42] Scott L. Nuismer, Andrew Basinski, and James J. Bull. Evolution and containment of transmissible recombinant vector vaccines. *Evolutionary Applications*, 12(8):1595–1609, 2019.
- [43] Scott Nuismer and James Bull. Self-disseminating vaccines to suppress zoonoses. *Nature Ecology & Evolution*, 4:1–6, 07 2020.
- [44] Nathan Layman, Beth M Tuschhoff, and Scott L Nuismer. Designing transmissible viral vaccines for evolutionary robustness and maximum efficiency. *Virus Evolution*, 01 2021.
- [45] Andrew J Basinski, Scott L Nuismer, and Christopher H Remien. A little goes a long way: Weak vaccine transmission facilitates oral vaccination campaigns against zoonotic pathogens. *PLOS Neglected Tropical Diseases*, 13(3):e0007251, 2019.
- [46] L. N. Farroway, G.R. Singleton, M. A. Lawson, and D. A. Jones. The impact of murine cytomegalovirus (MCMV) on enclosure populations of house mice (*Mus domesticus*). *Wildlife Research*, 29:11–17, 2002.
- [47] Joseph B. McCormick, Patricia A. Webb, John W. Krebs, Karl M. Johnson, and Ethleen S. Smith. A prospective study of the epidemiology and ecology of Lassa fever. *Journal of Infectious Diseases*, 155(3):437–444, 1987.

- [48] Kim Blasdell, Stuart Becker, Jane Hurst, Mike Begon, and Malcolm Bennett. Host range and genetic diversity of arenaviruses in rodents, United Kingdom. *Emerging Infectious Diseases*, 14:1455–8, 10 2008.
- [49] Ayodeji Olayemi, Akinlabi Oyeyiola, Adeoba Obadare, Joseph Igbokwe, Adetunji Adesina, Francis Onwe, Kingsley Ukwaja, Nnennaya Ajayi, Toni Rieger, Stephan Günther, and Elisabeth Fichet-Calvet. Widespread arenavirus occurrence and seroprevalence in small mammals, Nigeria. *Parasites & Vectors*, 11, 2018.
- [50] Scott L. Nuismer, Christopher H. Remien, Andrew J. Basinski, Tanner Varrelman, Nathan Layman, Kyle Rosenke, Brian Bird, Michael Jarvis, Peter Barry, Patrick W. Hanley, and Elisabeth Fichet-Calvet. Bayesian estimation of Lassa virus epidemiological parameters: Implications for spillover prevention using wildlife vaccination. *PLOS Neglected Tropical Diseases*, 14(9):1–20, 09 2020.
- [51] Valentina Tagliapietra, Roberto Rosà, Heidi Hauffe, Juha Laakkonen, Liina Voutilainen, Olli Vapalahti, Antti Vaheri, Heikki Henttonen, and Annapaola Rizzoli. Spatial and temporal dynamics of lymphocytic choriomeningitis virus in wild rodents, northern Italy. *Emerging Infectious Diseases*, 15:1019–25, 08 2009.
- [52] Philippe Mähl, Florence Cliquet, Anne-Laure Guiot, Enel Niin, Emma Fournials, Nathalie Saint-Jean, Michel Aubert, Charles Rupprecht, and Sylvie Gueguen. Twenty year experience of the oral rabies vaccine SAG2 in wildlife: A global review. *Veterinary Research*, 45:77, 08 2014.
- [53] M Val, Hansjürgen Volkmer, Jonathan Rothbard, Stipan Jonjic, Martin Messerle, J Schickedanz, M. Reddehase, and Ulrich Koszinowski. Molecular basis for cytolytic T-lymphocyte recognition of the murine cytomegalovirus immediate-early protein pp89. *Journal of Virology*, 62:3965–72, 12 1988.

- [54] Matthias Reddehase, Jonathan Rothbard, and Ulrich Koszinowski. A pentapeptide as minimal antigenic determinant for mhc class I-restricted T lymphocytes. *Nature*, 337:651–3, 03 1989.
- [55] Shelley Gorman, Nicole Harvey, Dorian Moro, Megan Lloyd, Valentina Voigt, Lee Smith, Malcolm Lawson, and Geoffrey Shellam. Mixed infection with multiple strains of murine cytomegalovirus occurs following simultaneous or sequential infection of immunocompetent mice. *Journal of General Virology*, 87:1123–32, 06 2006.
- [56] RM Anderson and RM May. *Infectious Diseases of Humans: Dynamics and Control*. Oxford University Press, 1992.
- [57] Megan Griffiths, Laura Bergner, Alice Broos, Diana Meza, Ana Filipe, Andrew Davison, Carlos Tello, Daniel Becker, and Daniel Streicker. Epidemiology and biology of a herpesvirus in rabies endemic vampire bat populations. *Nature Communications*, 11, 11 2020.
- [58] Shelley Gorman, Megan L. Lloyd, Lee M. Smith, Andrea R. McWhorter, Malcolm A. Lawson, Alec J. Redwood, and Geoffrey R. Shellam. Prior infection with murine cytomegalovirus (MCMV) limits the immunocontraceptive effects of an MCMV vector expressing the mouse zona-pellucida-3 protein. *Vaccine*, 26(31):3860–3869, 2008.
- [59] Sonia Nikolovski, Megan L. Lloyd, Nicole Harvey, Christopher M. Hardy, Geoffrey R. Shellam, and Alec J. Redwood. Overcoming innate host resistance to vaccination: Employing a genetically distinct strain of murine cytomegalovirus avoids vector-mediated resistance to virally vectored immunocontraception. *Vaccine*, 27(38):5226–5232, 2009.
- [60] L. N. Farroway, S. Gorman, M. A. Lawson, N. L. Harvey, D. A. Jones, G. R. Shellam, and G. R. Singleton. Transmission of two Australian strains of murine



- cytomegalovirus (MCMV) in enclosure populations of house mice (*Mus domesticus*). *Epidemiology and Infection*, 133(4):701–710, 08 2005.
- [61] Abigail Smith and Charles Krebs. The prevalence of viral antibodies during a large population fluctuation of house mice in Australia. *Epidemiology and Infection*, 125:719 – 727, 12 2000.
- [62] Alec Redwood, Lee Smith, Megan Lloyd, Lyn Hinds, Christopher Hardy, and Geoffrey Shellam. Prospects for virally vectored immunocontraception in the control of wild house mice (*Mus domesticus*). *Wildlife Research*, 34, 01 2007.
- [63] June E. Osborn. Cytomegalovirus and other herpesviruses. In Henry L. Foster, J. David Small, and James G. Fox, editors, *Diseases: The Mouse in Biomedical Research*, volume 2, chapter 13, pages 267 – 292. Academic Press, 1982.
- [64] A. D. Arthur, C. J. Krebs, R. P. Pech, L. N. Farroway, and G. R. Singleton. The transmission rate of MCMV in house mice in pens: implications for virally vectored immunocontraception. *Wildlife Research*, 36(5):386–393, 2009.
- [65] Mark A. Beaumont. Approximate Bayesian computation in evolution and ecology. *Annual Review of Ecology, Evolution, and Systematics*, 41(1):379–406, 2010.
- [66] Mikael Sunnåker, Alberto Giovanni Busetto, Elina Numminen, Jukka Corander, Matthieu Foll, and Christophe Dessimoz. Approximate Bayesian computation. *PLOS Computational Biology*, 9(1):1–10, 01 2013.
- [67] C. J. Clopper and E. S. Pearson. The use of confidence or fiducial limits illustrated in the case of the binomial. *Biometrika*, 26(4):404–413, 1934.
- [68] L. Ballenger. *Mus musculus*. [https://animaldiversity.org/accounts/Mus\\_musculus/](https://animaldiversity.org/accounts/Mus_musculus/), 1999.

- [69] Linda J.S. Allen. An introduction to stochastic epidemic models. In Fred Brauer, Jianhong Wu, and Pauline van den Driessche, editors, *Mathematical Epidemiology*, chapter 3, pages 93–94. Springer, 2008.
- [70] Andrea R. McWhorter, Lee M. Smith, Laura L. Masters, Baca Chan, Geoffrey R. Shellam, and Alec J. Redwood. Natural killer cell dependent within-host competition arises during multiple MCMV infection: Consequences for viral transmission and evolution. *PLOS Pathogens*, 9(1):1–13, 01 2013.
- [71] O Diekmann, JAP Heesterbeek, and JAJ Metz. On the definition and the computation of the basic reproduction ratio  $r_0$  in models for infectious diseases in heterogeneous populations. *Journal of Mathematical Biology*, 28(4):365–382, 1990.
- [72] Africa CDC. Lassa fever. <https://africacdc.org/disease/lassa-fever/>, 2021.
- [73] Edward H. Stephenson, Edgar W. Larson, and Joseph W. Dominik. Effect of environmental factors on aerosol-induced Lassa virus infection. *Journal of Medical Virology*, 14(4):295–303, 1984.
- [74] Ayodeji Olayemi, Dániel Cadar, Faly Magassouba, Adeoba Obadare, Fode Kourouma, Akinlabi Oyeyiola, Fasogbon Samuel Ayobami, Joseph Igbokwe, Toni Rieger, Sabrina Bockholt, Hanna Jerome, Jonas Schmidt-Chanasit, Mutien Garigliany, Stephan Lorenzen, Felix Igbahenah, Jean-Nicolas Fichet, Daniel Ortsega, Sunday Omilabu, Stephan Günther, and Elisabeth Fichet-Calvet. New hosts of the Lassa virus. *Scientific Reports*, 6, 05 2016.
- [75] Ayodeji Olayemi, Adeoba Obadare, Akinlabi Oyeyiola, Fasogbon Samuel Ayobami, Joseph Igbokwe, Felix Igbahenah, Daniel Ortsega, Stephan Günther, Erik Verheyen, and Elisabeth Fichet-Calvet. Small mammal diversity and dynamics within Nigeria, with emphasis on reservoirs of the Lassa virus. *Systematics and Biodiversity*, 16:1–10, 08 2017.

- [76] Elisabeth Fichet-Calvet and David John Rogers. Risk maps of Lassa fever in West Africa. *PLOS Neglected Tropical Diseases*, 3(3):1–13, 03 2009.
- [77] Andrew J. Basinski, Elisabeth Fichet-Calvet, Anna R. Sjodin, Tanner J. Varrelman, Christopher H. Remien, Nathan C. Layman, Brian H. Bird, David J. Wolking, Corina Monagin, Bruno M. Ghersi, Peter A. Barry, Michael A. Jarvis, Paul E. Gessler, and Scott L. Nuismer. Bridging the gap: Using reservoir ecology and human serosurveys to estimate Lassa virus spillover in West Africa. *PLOS Computational Biology*, 17(3):1–24, 03 2021.
- [78] Sebastien Kenmoe, Serges Tchatchouang, Jean Thierry Ebogo-Belobo, Aude Christelle Ka’e, Gadji Mahamat, Raïssa Estelle Guiamdjo Simo, Arnol Bowo-Ngandji, Cynthia Paola Demeni Emoh, Emmanuel Che, Dimitri Tchami Ngongang, Marie Amougou-Atsama, Nathalie Diane Nzukui, Chris Andre Mbongue Mikangue, Donatien Serge Mbagha, Sorel Kenfack, Sandrine Rachel Kingue Bebey, Nathalie Amvongo Adjia, Atembeh Noura Efietngab, Hervé Raoul Tazokong, Abdou Fatawou Modiyinji, Cyprien Kengne-Nde, Serge Alain Sadeuh-Mba, and Richard Njouom. Systematic review and meta-analysis of the epidemiology of Lassa virus in humans, rodents and other mammals in sub-Saharan Africa. *PLOS Neglected Tropical Diseases*, 14(8):1–29, 08 2020.
- [79] Donald S. Grant, Humarr Khan, John Schieffelin, and Daniel G. Bausch. Chapter 4 - Lassa fever. In Önder Ergönül, Füsün Can, Lawrence Madoff, and Murat Akova, editors, *Emerging Infectious Diseases*, pages 37–59. Academic Press, Amsterdam, 2014.
- [80] P Huston, VL Edge, and E Bernier. Reaping the benefits of open data in public health. *Canada Communicable Disease Report*, 45:252–256, 10 2019.

- [81] Karen Clark, Ilene Karsch-Mizrachi, David J Lipman, James Ostell, and Eric W Sayers. Genbank. *Nucleic Acids Research*, 44(D1):D67–D72, 01 2016.
- [82] Michael Widenius, Davis Axmark, and Paul DuBois. *Mysql Reference Manual*. O’Reilly & Associates, Inc., USA, 1st edition, 2002.
- [83] Miguel Grinberg. *Flask web development: developing web applications with python*. O’Reilly Media, Inc., 2018.
- [84] Guido Van Rossum and Fred L. Drake. *Python 3 Reference Manual*. CreateSpace, Scotts Valley, CA, 2009.
- [85] David Flanagan. *JavaScript: the definitive guide*. O’Reilly Media, Inc., 2006.
- [86] Karan Patel. Incremental journey for world wide web: introduced with web 1.0 to recent web 5.0—a survey paper. *International Journal of Advanced Research in Computer Science and Software Engineering*, 3(10), 2013.
- [87] Vladimir Agafonkin. Leaflet (1.7.1), 2021.
- [88] Plotly Technologies Inc. Collaborative data science, 2015.
- [89] David W. Fraser, C. Clinton Campbell, Thomas P. Monath, Paul A. Goff, and Michael B. Gregg. Lassa fever in the eastern province of Sierra Leone, 1970–1972: I. epidemiologic studies. *The American Journal of Tropical Medicine and Hygiene*, 23(6):1131 – 1139, 01 Nov. 1974.
- [90] J. E. Yalley-Ogunro, J. D. Frame, and A. P. Hanson. Endemic Lassa fever in Liberia. VI. Village serological surveys for evidence of Lassa virus activity in Lofa County, Liberia. *Transactions of The Royal Society of Tropical Medicine and Hygiene*, 78(6):764–770, 01 1984.

- [91] I. S. Lukashevich, J. C. S. Clegg, and K. Sidibe. Lassa virus activity in Guinea: Distribution of human antiviral antibody defined using enzyme-linked immunosorbent assay with recombinant antigen. *Journal of Medical Virology*, 40(3):210–217, 1993.
- [92] Solen Kernéis, Lamine Koivogui, N’Faly Magassouba, Kekoura Koulemou, Rosamund Lewis, Aristide Aplogan, Rebecca F. Grais, Philippe J. Guerin, and Elisabeth Fichet-Calvet. Prevalence and risk factors of Lassa seropositivity in inhabitants of the forest region of Guinea: A cross-sectional study. *PLOS Neglected Tropical Diseases*, 3(11):1–9, 11 2009.
- [93] Shirley C. Nimo-Paintsil, Elisabeth Fichet-Calvet, Benny Borremans, Andrew G. Letizia, Emad Mohareb, Joseph H. K. Bonney, Kwasi Obiri-Danso, William K. Ampofo, Randal J. Schoepp, and Karl C. Kronmann. Rodent-borne infections in rural Ghanaian farming communities. *PLOS ONE*, 14(4):1–13, 04 2019.
- [94] Nafomon Sogoba, Kyle Rosenke, Jennifer Adjemian, Sory Ibrahim Diawara, Ousmane Maiga, Moussa Keita, Drissa Konaté, Abdoul Salam Keita, Ibrahim Sissoko, Matt Boisen, Diana Nelson, Darin Ottamasathien, Molly Millett, Robert F Garry, Luis M Branco, Sékou F Traoré, Seydou Doumbia, Heinz Feldmann, and David Safronetz. Lassa virus seroprevalence in Sibirilia commune, Bougouni district, southern Mali. *Emerging Infectious Diseases*, 22(4):657–663, 04 2016.
- [95] H Wulff, A Fabiyi, and T P Monath. Recent isolations of Lassa virus from Nigerian rodents. *Bulletin of the World Health Organization*, 52(4-6):609–613, 1975.
- [96] Thomas P. Monath, Verne F. Newhouse, Graham E. Kemp, Henry W. Setzer, and Anthony Cacciapuoti. Lassa virus isolation from *Mastomys natalensis* rodents during an epidemic in Sierra Leone. *Science*, 185(4147):263–265, 1974.

- [97] Elisabeth Fichet-Calvet, Beate Becker-Ziaja, Lamine Koivogui, and Stephan Günther. Lassa serology in natural populations of rodents and horizontal transmission. *Vector-Borne and Zoonotic Diseases*, 14:665–674, 09 2014.
- [98] Emilie Lecompte, Elisabeth Fichet-Calvet, Stéphane Daffis, Kékoura Koulémou, Oumar Sylla, Fodé Kourouma, Amadou Doré, Barré Soropogui, Vladimir Aniskin, Bernard Allali, Stéphane Kouassi Kan, Aude Lalis, Lamine Koivogui, Stephan Günther, Christiane Denys, and Jan ter Meulen. *Mastomys natalensis* and Lassa fever, West Africa. *Emerging Infectious Diseases*, 12(12):1971–1974, 12 2006.
- [99] David Coulibaly-N’Golo, Bernard Allali, Stéphane K. Kouassi, Elisabeth Fichet-Calvet, Beate Becker-Ziaja, Toni Rieger, Stephan Ölschläger, Henri Dosso, Christiane Denys, Jan ter Meulen, Chantal Akoua-Koffi, and Stephan Günther. Novel arenavirus sequences in *Hylomyscus* sp. and *Mus (Nannomys) setulosus* from Côte d’Ivoire: Implications for evolution of arenaviruses in Africa. *PLOS ONE*, 6(6):1–9, 06 2011.
- [100] David Safronetz, Job E Lopez, Nafomon Sogoba, Sékou F Traore’, Sandra J Raffel, Elizabeth R Fischer, Hideki Ebihara, Luis Branco, Robert F Garry, Tom G Schwan, and Heinz Feldmann. Detection of Lassa virus, Mali. *Emerging Infectious Diseases*, 16(7):1123–1126, 07 2010.
- [101] David Safronetz, Nafomon Sogoba, Job E. Lopez, Ousmane Maiga, Eric Dahlstrom, Marko Zivcec, Friederike Feldmann, Elaine Haddock, Robert J. Fischer, Jennifer M. Anderson, Vincent J. Munster, Luis Branco, Robert Garry, Stephen F. Porcella, Tom G. Schwan, and Heinz Feldmann. Geographic distribution and genetic characterization of Lassa virus in sub-Saharan Mali. *PLOS Neglected Tropical Diseases*, 7(12):1–9, 12 2013.

- [102] Karl C Kronmann, Shirley Nimo-Paintsil, Fady Guirguis, Lisha C Kronmann, Kofi Bonney, Kwasi Obiri-Danso, William Ampofo, and Elisabeth Fichet-Calvet. Two novel arenaviruses detected in pygmy mice, Ghana. *Emerging Infectious Diseases*, 19(11):1832–1835, 11 2013.
- [103] Yadouleton Angès, Achaz Agolinou, Fodé Kourouma, Raoul Saizonou, Meike Pahlmann, Sonia Bedié, Honoré Bankolé, Beate Becker-Ziaja, Fernand Gbaguidi, Anke Thielebein, N’Faly Magassouba, Sophie Duraffour, Jean-Pierre Baptiste, Stephan Günther, and Elisabeth Fichet-Calvet. Lassa virus in pygmy mice, Benin, 2016-2017. *Emerging Infectious Diseases*, 25:1977–1979, 10 2019.
- [104] M D Bowen, P E Rollin, T G Ksiazek, H L Hustad, D G Bausch, A H Demby, M D Bajani, C J Peters, and S T Nichol. Genetic diversity among Lassa virus strains. *Journal of Virology*, 74(15):6992–7004, 08 2000.
- [105] David D. Auperin, Donna R. Sasso, and Joseph B. McCormick. Nucleotide sequence of the glycoprotein gene and intergenic region of the Lassa virus S genome RNA. *Virology*, 154(1):155–167, 1986.
- [106] J.C.S. Clegg and J.D. Oram. Molecular cloning of Lassa virus RNA: Nucleotide sequence and expression of the nucleocapsid protein gene. *Virology*, 144(2):363–372, 1985.
- [107] Simon Vieth, Andrew E. Torda, Marcel Asper, Herbert Schmitz, and Stephan Günther. Sequence analysis of L RNA of Lassa virus. *Virology*, 318(1):153–168, 2004.
- [108] Elisabeth Fichet-Calvet, Stephan Ölschläger, Thomas Strecker, Lamine Koivogui, Beate Becker-Ziaja, Amara Camara, Barré Soropogui, N’Faly Magassouba, and Stephan Günther. Spatial and temporal evolution of Lassa virus in the natural host population in upper Guinea. *Scientific Reports*, 6:21977, 02 2016.

- [109] Stephan Olschläger, Michaela Lelke, Petra Emmerich, Marcus Panning, Christian Drosten, Meike Hass, Danny Asogun, Deborah Ehichioya, Sunday Omilabu, and Stephan Günther. Improved detection of Lassa virus by reverse transcription-pcr targeting the 5' region of s rna. *Journal of Clinical Microbiology*, 48(6):2009–2013, 06 2010.
- [110] Deborah U Ehichioya, Meike Hass, Stephan Olschläger, Beate Becker-Ziaja, Christian O Onyebuchi Chukwu, Jide Coker, Abdulsalam Nasidi, Osi Ogbu Ogugua, Stephan Günther, and Sunday A Omilabu. Lassa fever, Nigeria, 2005-2008. *Emerging Infectious Diseases*, 16(6):1040–1041, 06 2010.
- [111] Deborah U. Ehichioya, Meike Hass, Beate Becker-Ziaja, Jacqueline Ehimuan, Danny A. Asogun, Elisabeth Fichet-Calvet, Katja Kleinsteuber, Michaela Lelke, Jan ter Meulen, George O. Akpede, Sunday A. Omilabu, Stephan Günther, and Stephan Ölschläger. Current molecular epidemiology of Lassa virus in Nigeria. *Journal of Clinical Microbiology*, 49(3):1157–1161, 2011.
- [112] Danny A. Asogun, Donatus I. Adomeh, Jacqueline Ehimuan, Ikponmwonsa Odia, Meike Hass, Martin Gabriel, Stephan Ölschläger, Beate Becker-Ziaja, Onikepe Folarin, Eric Phelan, Philomena E. Ehiane, Veritas E. Ifeh, Eghosasere A. Uyigüe, Yemisi T. Oladapo, Ekene B. Muoebonam, Osagie Osunde, Andrew Dongo, Peter O. Okokhere, Sylvanus A. Okogbenin, Mojeed Momoh, Sylvester O. Alikah, Odigie C. Akhuemokhan, Peter Imomeh, Maxy A. C. Odike, Stephen Gire, Kristian Andersen, Pardis C. Sabeti, Christian T. Happi, George O. Akpede, and Stephan Günther. Molecular diagnostics for Lassa fever at Irrua Specialist Teaching Hospital, Nigeria: Lessons learnt from two years of laboratory operation. *PLOS Neglected Tropical Diseases*, 6(9):1–14, 09 2012.
- [113] Tomasz A Leski, Michael G Stockelman, Lina M Moses, Matthew Park, David A Stenger, Rashid Ansumana, Daniel G Bausch, and Baochuan Lin. Sequence vari-



- ability and geographic distribution of Lassa virus, Sierra Leone. *Emerging Infectious Diseases*, 21(4):609–618, 04 2015.
- [114] S Atkin, S Anaraki, P Gothard, A Walsh, D Brown, R Gopal, J Hand, and D Morgan. The first case of Lassa fever imported from Mali to the United Kingdom, February 2009. *Eurosurveillance*, 14(10), 2009.
- [115] Ayodeji Olayemi, Adeoba Obadare, Akinlabi Oyeyiola, Joseph Igbokwe, Fasogbon Samuel Ayobami, Felix Igbahenah, Daniel Ortsega, Danny Asogun, Prince Umeh, Innocent Vakkai, Abejegah Chukwuyem, Meike Pahlmann, Beate Becker-Ziaja, Stephan Günther, and Elisabeth Fichet-Calvet. Arenavirus diversity and phylogeography of *Mastomys natalensis* rodents, Nigeria. *Emerging Infectious Diseases*, 22, 04 2016.
- [116] Anges Yadouleton, Caroline Picard, Toni Rieger, Frederic Loko, Daniel Cadar, Emile Cossi Kouthon, Emmanuel Obolli Job, Honoré Bankolé, Lisa Oestereich, Fernand Gbaguidi, Meike Pahlman, Beate Becker-Ziaja, Alexandra Journeaux, Delphine Pannetier, Stéphane Mély, Stéphanie Mundweiler, Damien Thomas, Leon Kohossi, Raoul Saizonou, Clement Glele Kakai, Magloire Da Silva, Sonia Kossoubedie, AndréLukusa Kakonku, Pierre M’Pelé, Stephan Günther, Sylvain Baize, and Elisabeth Fichet-Calvet. Lassa fever in Benin: description of the 2014 and 2016 epidemics and genetic characterization of a new Lassa virus. *Emerging Microbes & Infections*, 9(1):1761–1770, 12 2020.
- [117] Elsie A Ilori, Christina Frank, Chioma C Dan-Nwafor, Oladipupo Ipadeola, Amrei Krings, Winifred Ukponu, Oboma E Womi-Eteng, Ayodele Adeyemo, Samuel K Mutbam, Emmanuel O Musa, Clement L P Lasuba, Wondimagegnehu Alemu, Sylvanus Okogbenin, Ephraim Ogbaini, Uche Unigwe, Emeka Ogah, Robinson Onoh, Chukwuyem Abejegah, Olufemi Ayodeji, and Chikwe Ihekweazu. Increase

in Lassa fever cases in Nigeria, January-March 2018. *Emerging Infectious Diseases*, 25(5):1026–1027, 05 2019.